Degradation of a novel DNA damage response protein, tankyrase 1 binding protein 1, following adenovirus infection

Chalabi Hagkarim, Nafiseh; Ryan, Ellis; Byrd, Philip; Hollingworth, Robert; Shimwell, Neil; Agathanggelou, Angelo; Vavasseur, Manon; Kolbe, Viktoria; Speisder, Thomas ; Dobner, Thomas ; Stewart, Grant; Grand, Roger

DOI:
10.1128/JVI.02034-17

1 Degradation of a novel DNA damage response protein, tankyrase 1 binding protein 1 (Tab182),

2 following adenovirus infection.

3

4 Nafiseh Chalabi Hagkarim[1, 3], Ellis L. Ryan[1, 3, 4], Philip J. Byrd[1], Robert Hollingworth[1], Neil J.

5 Shimwell[1], Angelo Agathanggelou[1], Manon Vavasseur[1], Viktoria Kolbe[2], Thomas Speiseder[2], Thomas

6 Dobner[2], Grant S. Stewart[1]* and Roger J. Grand[1]*

7 [1]Institute of Cancer and Genomic Sciences,

8 College of Medicine and Dentistry,

9 University of Birmingham,

10 Birmingham, U.K. B15 2TT

11 [2] Heinrich Pette Institute,

12 Leibniz Institute for Experimental Virology,

13 Hamburg, Germany

14 [3] These authors made equal contribution to this work.

15 [4] Present address: Centre for Mechanochemical Cell Biology

16 Warwick Medical School

17 University of Warwick

18 *corresponding authors, r.j.a.grand@bham.ac.uk telephone 44 121 414 2805,

19 g.s.stewart@bham.ac.uk telephone 44 121 414 9168

20

21 Running title: Adenoviruses target Tab182 for degradation.

22 Keywords: adenovirus, adenovirus E1B55K, Tab182, TNKS1BP1, CNOT complex, CNOT1

23 Abstract 249 words

24 Importance 149 words

Abstract

Infection by most DNA viruses activates a cellular DNA damage response (DDR), which may be to the detriment or advantage of the virus. In the case of adenoviruses, they neutralise anti-viral effects of DDR activation by targeting a number of proteins for rapid proteasome-mediated degradation. We have now identified a novel DDR protein, tankyrase 1 binding protein 1 (TNKS1BP1 also known as Tab182), which is degraded during infection by adenovirus 5 and adenovirus 12. In both cases, degradation requires the action of E1B55K and E4orf6 viral proteins and is mediated through the proteasome by the action of cullin-based cellular E3 ligases. The degradation of Tab182 appears to be serotype specific as the protein remains relatively stable following infection with adenoviruses 4, 7, 9 and 11. We have gone on to confirm that Tab182 is an integral component of the CNOT complex, which has transcriptional regulatory, deadenylation and E3 ligase activity. At least 2 other members of the complex (CNOT3 and CNOT7) are also reduced in level during adenovirus infection whereas levels of CNOT4 and CNOT1 remain stable. Depletion of Tab182 with siRNA enhances expression of E1As to a limited extent during adenovirus infection but depletion of CNOT1 is particularly advantageous to the virus and results in a marked increase in expression of adenovirus early proteins. In addition, depletion of Tab182 and CNOT1 results in a limited increase in viral DNA during infection. We conclude that the cellular CNOT complex is a previously unidentified major target for adenoviruses during infection.

Importance

Adenoviruses target a number of cellular proteins involved in the DNA damage response for rapid degradation. We have now shown that Tab182, which we have confirmed to be an integral component of the mammalian CNOT complex, is degraded following infection by adenovirus serotypes 5 and 12. This requires the viral E1B55K and E4orf6 proteins and is mediated by cullin-based E3 ligases and the proteasome. In addition to Tab182, other CNOT proteins are also reduced during adenovirus infection. Thus, CNOT3 and CNOT7, for example, are degraded whereas CNOT4 and CNOT1 are not. siRNA-mediated depletion of components of the complex enhances the

expression of adenovirus early proteins and increases the concentration of viral DNA produced during infection. This study highlights a novel protein complex, CNOT, which is targeted for adenovirus-mediated protein degradation. To our knowledge this is the first time that the CNOT complex has been identified as an adenoviral target.

Introduction

Adenoviruses are, together with the Papilloma and Polyoma viruses, members of the small DNA tumour virus family (1). There are in excess of 70 human adenovirus types, subdivided into 7 species, designated A-G; the most commonly studied are the group C adenoviruses types 2 and 5 (Ad2 and Ad5) and the group A oncogenic adenovirus 12 (Ad12). Adenoviruses have a linear double-stranded DNA genome, approximately 35kbp in length. The first gene to be expressed, following infection, is adenovirus early region 1A (AdE1A) which is present in two major forms-a long form and a short form translated from 13S and 12S mRNAs, respectively. AdE1A induces progression of the host cell into a 'pseudo-S-phase' through interaction with a number of cellular proteins, such as the Rb family, CBP/p300 and components of the cellular transcriptional machinery (2-4). It is considered that this provides an environment conducive to viral replication. Adenovirus E1A is the major adenovirus oncogene and has long been known to transform cells in culture in combination with a co-operating oncogene, such mutant Ras or adenovirus E1B (3, 5).

Shortly after initial infection the host cell initiates a DNA damage response (DDR), seen as phosphorylation of a number of well-characterised Ataxia telangiectasia mutated (ATM) and ATM and Rad3-related (ATR) substrates (6-8). It is presumed that this may be due to recognition of the viral genome as broken cellular DNA or perhaps due to stress caused by infection itself. The virus, in turn, is able to inhibit the DDR, primarily by degradation and/or mis-localization of its key components (7-12). The cellular DDR comprises a series of pathways which have evolved to deal with different forms of DNA damage, such as double strand breaks (DSBs), single strand breaks (SSBs), and the formation of bulky adducts and base mismatches (13-15). The response to DSBs is largely based on the activities of three kinases – ATM, ATR, and DNA dependent protein kinase

(DNA-PK). DSBs can be detected by both the MRN complex (comprising MRE11, Rad50 and NBS1) or the Ku 70/80 heterodimer which can lead to repair by homologous recombination (HR) or non-homologous end joining (NHEJ), respectively. Recognition of DSBs by MRN is followed by the recruitment of ATM, which is activated by acetylation by Tip60 while binding of Ku70/80 results in auto-phosphorylation of DNA-PK that is required for NHEJ (16-18). Histone H2AX and multiple down-stream targets are phosphorylated by ATM which has the effect of recruiting a large number of components to the lesion to initiate repair, as well as to cause cell cycle arrest so that damaged DNA is not replicated (13-17). ATR is activated in response to single-stranded DNA (ssDNA) which can arise as a result of DSB repair and stalled replication forks. Regions of ssDNA are coated with replication protein A (RPA) which, in turn, recruits ATR and the ATR interacting protein, ATRIP. Further complexes, comprising Rad9-Rad1 and Hus1 (9-1-1) and Rad17-replication factor C2 (RFC2) clamp loader, together with TOPBP1 are recruited to ssDNA, RPA and ATR leading to cell cycle arrest and repair (17-19).

It was originally shown that when cells were infected with a mutant Ad5 virus, lacking the E4 region, viral genomes were joined end to end to form concatamers which could not be packaged into viral capsids (20). It was later demonstrated that during infection with *wt* virus, cellular E3 ligases are hi-jacked by the virus and used to degrade key cellular DDR proteins; for example, p53 is degraded by both Ad5 and Ad12 and requires the action of the E1B55K and E4orf6 viral proteins (21-23). In the case of Ad5 the viral proteins recruit an E3 ligase, comprising elongins B and C, Rbx and cullin 5, which ubiquitylates p53 and this is then degraded by the proteasome (9). Similarly, Ad12 also facilitates the degradation of p53, but through a cullin 2-based E3 ligase (12). Other DDR proteins degraded during Ad5 and Ad12 infection include MRE11, DNA ligase IV and BLM (10, 11, and 24). In addition to DDR components a number of other unrelated proteins are also degraded during Ad5 infection. These substrates include DAXX, integrin3α and TIF1γ (25-27). During infection adenoviruses also cause translocation of proteins associated with the DDR. For example, ATR, ATRIP, Rad 17, 53BP1, BRCA1, TOPBPI, RPA and hnRNPUL-1 have all been observed at sites of viral

replication in the nucleus, known as viral replication centres (VRCs) (6, 8 and 28). In addition, it is notable that certain DDR proteins, such as p53 and MRE11, are translocated to aggresomes where they may be degraded (29-31).

Tab182 (also known as tankyrase 1 binding protein 1 [TNKS1BP1]) has previously been shown to be an ATM and/or ATR substrate which is highly phosphorylated following exposure to ionizing radiation (IR) and to bind to tankyrase 1 (32, 33). It appears to be required for efficient DSB repair and facilitates PARP1-dependent autophosphorylation of DNA-PK although its precise role is not clear at present (34, 35 and our unpublished data). In addition, Tab182 has a role in regulation of the actin cytoskeleton (36). Tab182 has previously been suggested to be a component of the mammalian CNOT complex although its role in that context is unknown. The CNOT complex is a multi-protein complex, highly conserved in eukaryotes (37-39). In humans, the CNOT complex is composed of components CNOT1 to 11 (CNOT9 and CNOT11 have the alternative nomenclature RQCD and C2orf29, respectively) (40, 41). In yeast, where most studies of CCR4-NOT have been performed, there are 9 core subunits-Cer4, Caf1, Caf40, Caf130 and NOTs1-5, although no Tab182 ortholog has been identified (38, 42 and 43). The human CNOT complex consists of a stable inner complex (CNOT1, CNOT2, CNOT3, CNOT9 and CNOT10) with CNOT6 and its homologue 6L, CNOT7 and CNOT8 being less strongly associated. CNOT4 seems to be weakly associated, whereas Tab182 and C2orf29 (CNOT11) are more strongly bound (40, 44 and 45). Many different enzymatic activities have been attributed to the CCR4-NOT complex in yeast and CNOT in mammals. It is considered to be a major deadenylase, responsible, with Pan2-Pan3, for shortening of the poly (A) tails of cytoplasmic RNAs (38, 46 and 47). The components CNOT7 and CNOT8, together with CNOT6 and CNOT6L, are deadenylase subunits. Further components of the complex have E3 ligase, translational repression, RNA export and nuclear surveillance activities (38, 48-50). CNOT4 is the E3 ubiquitin ligase but seems to interact only weakly with the remainder of the complex (40). CNOT1 forms a scaffold on which the CNOT and deadenylase modules are formed (41, 51 and 52). The central region of CNOT1 interacts with the deadenylase subunits, with CNOT7 forming a bridge between CNOT1 and CNOT6L

(39). The C-terminal region of CNOT1 binds to the remainder of the NOT module which comprises CNOT2 and CNOT3.

A number of studies have implicated the CCR4-NOT complex in the DDR in yeast. In the majority of these, sensitivity assays were performed using yeast strains that were mutant for various CCR4-NOT components. For example, loss of CCR4 and Caf1 render the yeast sensitive to IR, hydroxyurea (HU) and camptothecin, an inhibitor of DNA topoisomerase I (53-55). Similarly, NOT1-5 mutant yeast strains have been shown to be sensitive to HU (53). These data suggest that the CCR4-NOT complex is involved in the response to a number of forms of DNA damage and replication stress although the mechanisms involved remain unclear.

Here we demonstrate that Tab182 is degraded during Ad5 and Ad12 infection in an E1B55K- and E4orf6-dependent manner. We have confirmed that Tab182 is a component of the CNOT complex and that levels of at least two other components of the complex are similarly reduced during adenovirus infection. Significantly, depletion of Tab182 or disruption of the CNOT complex enhances expression of adenovirus E1A at the transcriptional level early in infection.

Results

Tab182 is degraded during adenovirus infection.

It has previously been suggested that Tab182 may have a role in the DDR based on the observation that the protein has multiple potential ATM/ATR phosphorylation sites (SQ/TQ) and is phosphorylated following exposure to IR (33) as well as its recently proposed role in DSB repair (34, 35). In a screen to detect novel DDR components targeted by adenoviruses the effect of viral infection on Tab182 was examined. It can be seen that, during both Ad5 and Ad12 infection of HeLa cells, Tab182 levels decline rapidly after 24 hours (Figures 1A and 1B). It is particularly notable that the levels of Tab182 increase in the initial stages of infection with both serotypes (Figure 1 and succeeding figures). This appears to be a cell cycle effect, since, in nocodazole 'shake off' experiments, Tab182 expression is greatest during S phase and mitosis and reduced in the G1 phase

of the cell cycle (data not shown). RT-PCR analysis has demonstrated that the increased protein expression coincides with increases in Tab182 mRNA (data not shown).

Tab182 degradation requires the E1B55K and E4orf6 viral proteins

Multiple previous studies have demonstrated the roles of AdE1B55K and AdE4orf6 in targeting cellular proteins for degradation (6-12). To determine whether these components are involved in the observed reduction in level of Tab182, infection with a panel of mutant viruses was carried out. Infection with the Ad5 (Ad5 *dl*1520) and Ad12 (Ad12*dl*620) EIB55K negative viruses had no effect on the level of Tab182 (Figures 1C and 1D), indicating a requirement for the larger AdE1B protein for degradation.

Following infection with various Ad5E4 negative viruses there was no reduction in Tab182 level when the E4orf6 protein was not expressed, as in H5*pm*4154 and H5*pm*4155 (Figures 2A and 2B). Viruses which fail to express other E4 proteins degrade Tab182 in a manner comparable to wild type (Figure 2). Thus, H5*in*351 (E4orf1-), H5*in*352 (E4orf2-), H5*pm*4166 (E4orf4-) and H5*pm*4150 (E4orf3-) are all able to cause rapid degradation of Tab182 (Figure 2). The H5*dl*356 virus, which is E4orf7 negative, appears to express E4orf6 at much lower levels than expected which probably explains why levels of Tab182 and MRE11 are only very marginally reduced (Figure 2C). H5*pm*4155, which is E4orf3 and E4orf6 negative, expresses somewhat reduced levels of E1B55K, compared to the other viruses shown here (Figure 2C). Reasons for this are not apparent. Overall, we conclude that degradation of Tab182 requires, in Ad5 at least, E1B55K and E4orf6. Significantly, in all western blots shown in Figures 1 and 2 (and Figure 5A) degradation of Tab182 occurs somewhat later than degradation of MRE11 but at similar times to p53 degradation (data not shown).

In addition, to confirm that reduction in Tab182 levels is not due to a reduction in mRNA, RT-PCR was carried out on Ad5 and Ad12 infected cells (Figure 3). This clearly shows that Tab182 mRNA levels are equivalent to, or higher than, uninfected cells up to about 72 hours post infection in contrast to the sharp reduction in Tab182 protein levels after 24 hours (compare Figures 1 and 3).

179 We conclude that loss of Tab182 protein is due to active protein degradation and not host cell shut-
180 off which may occur after 72 hours (Figures 3A and 3B).

181 To demonstrate that the E1B55K and E4orf6 proteins are solely responsible for degradation of
182 Tab182 plasmids encoding the two Ad5 and Ad12 proteins were transfected into HeLa cells. Cells
183 were harvested after 48 hours and lysates subjected to western blotting for Tab182, MRE11 and the
184 viral proteins (Figure 4). E4orf6 proteins were HA-tagged and were detected with an anti-HA
185 antibody. It can be seen that Tab182 and MRE11 were degraded in the presence of both Ad5 and
186 Ad12 E1B55K and E4orf6 proteins. These data confirm that similar viral proteins are required for
187 both Ad5- and Ad12-mediated degradation of Tab182. When the viral proteins were expressed
188 singly there was little reduction in Tab182 or MRE11 levels confirming that both E1B55K and E4orf6
189 are required for degradation (Figure 4).

190 *Degradation of Tab182 is limited to certain virus serotypes*.

191 To determine how widespread the degradation of Tab182 is amongst other adenovirus serotypes,
192 levels of Tab182 were monitored by western blotting following infection of HeLa cells with Ad4
193 (group E), Ad7 (group B1), Ad9 (group D) and Ad11 (group B2) (Figure 5). In contrast to Ad5 and
194 Ad12, infection of HeLa cells with Ad9 and Ad11 viruses had no effect on Tab182 expression except
195 at very late times when host cell shut off could be a contributory factor (Figures 5B and 5C).
196 Following Ad4 and Ad7 infection there is a reduction in Tab182 levels at later times and this is more
197 pronounced than the effects seen with Ad9 and Ad11 but much less marked than degradation after
198 Ad5 and Ad12 infection (Figures 5B and 5C). The effects of the viruses on Tab182 levels closely
199 mirror those on MRE11 and, in the case of Ad4, on p53 (Figure 5). (Ad7, Ad9 and Ad11 all markedly
200 induce expression of p53 as has been reported earlier (28 and 56)). We have previously reported
201 that Ad4 facilitates rapid degradation of various DDR proteins (28) although perhaps to a lesser
202 extent than Ad5 and Ad12. However, it appears to have only a relatively slight effect on Tab182
203 (Figure 5B). Whilst there is limited reduction in protein level, it seems likely that the group B1, B2, D
204 and E viruses do not cause significant degradation of Tab182.

205 *Degradation of Tab182 requires the proteasome and E3 ligases.*

206 A number of approaches were adopted to investigate the mechanism by which target proteins are
207 degraded during Ad5 and Ad12 infection. Initially, to confirm that the degradation of Tab182 is by
208 the proteasome, cells were treated with bortezomib, a well-characterised proteasome inhibitor, or
209 DMSO (as a negative control) and harvested after 48 hours. In the presence of bortezomib
210 degradation of Tab182 and MRE11, following viral infection, was reduced but not completely
211 inhibited; in the absence of the proteasome inhibitor (DMSO) the proteins were degraded in the
212 presence of the viruses (Figure 6). In a second experiment it has been shown that inhibition of
213 NEDDylation (with MLN4924) also results in stabilisation of Tab182 following Ad5 and Ad12
214 infection. It is now well-established that NEDDylation is required for activation of the cullin
215 components of the E3 ligases during adenovirus infection (9). In the presence of the inhibitor,
216 degradation of Tab182 was appreciably reduced as was that of p53, although it is interesting to note
217 that stabilization of MRE11 was appreciably less than was the case for p53; this apparent differential
218 may be due to the up-regulation of p53 expression due to AdE1A (Figure 7A and 7B). The active
219 NEDDylated component of the cullin 2 can be seen as a slower migrating protein in the western blots
220 shown in Figures 7A and 7B. This is markedly reduced in the MLN4924 treated samples. We conclude
221 that active (NEDDylated) cullins are required for Tab182 degradation during adenovirus infection.
222 Different adenovirus serotypes do not all make use of the same cullin components to degrade
223 cellular proteins. Previously it has been shown that protein degradation following Ad5 infection
224 utilizes a cullin 5-based E3 ligase whereas Ad12 hijacks a cullin 2-based E3 ligase (9 and 12). To
225 examine whether this difference extends to the degradation of Tab182, H1299 cells, in which Cul2 or
226 Cul5 expression had been ablated, were infected with Ad5 and Ad12 and levels of Tab182 monitored
227 (Figures 7C, 7D and 7E). In the Cul2-negative cells Tab182 is more stable following Ad12 infection
228 compared with the control cell line indicating that Cul2 is required for degradation of Tab182 by this
229 serotype (Figures 7D and 7C). In contrast, in the Cul5-negative cells Tab182 levels are comparable
230 with control cells following Ad12 infection indicating that this cullin component is dispensable for

231 Tab182 degradation (Figures 7E and 7C). However, more subtle differences were observed between
232 the degradation of Tab182, after Ad5 infection, in the Cul2-negative and Cul5-negative cells (Figures
233 7D and 7E). During Ad5 infection the loss of either cullin may result in some stabilization of Tab182
234 compared to control H1299 cells but does not clearly abrogate its degradation (Figures 7C, 7D and
235 7E). As expected MRE11 is stabilized in the Cul5-negative cells but not the Cul2-negative cells after
236 Ad5 infection. This suggests the possible involvement of Cul2, and/or perhaps an unidentified cullin,
237 in Ad5-mediated Tab182 degradation. Further work will be required to determine if other proteins
238 beside cullins 2 and 5 are involved in protein degradation by Ad5.

239 *Tab182 does not localize to viral replication centres*

240 It has previously been shown that a number of DDR proteins localize to the sites of adenovirus
241 replication in the nucleus, known as viral replication centres (VRCs) (6 and 8). To examine if this
242 applied to Tab182, HeLa cells were transfected with GFP-Tab182 and left for 24 hours. They were
243 then seeded onto glass coverslips and infected with Ad5 or Ad12. After a further 24 hours cells were
244 fixed and stained with antibodies that recognise VRCs (Figure 8). In the case of Ad5, VRCs were
245 visualised using an antibody against the viral DNA binding protein (DBP) while RPA-32 was used as a
246 surrogate marker for Ad12 VRCs. No specific recruitment of Tab182 to viral replication centres was
247 observed following infection with either adenovirus serotype (Figure 8A). As expression of GFP-
248 Tab182 was greater than is the case for the *wt* protein, in a further experiment soluble proteins
249 were extracted before antibody staining; again no co-localisation of GFP-Tab182 with VRCs was
250 observed (Figure 8B).

251 *Tab182 associates with AdE1B55K proteins.*

252 As the adenovirus-mediated degradation of Tab182 is AdE1B55K dependent we investigated
253 whether the two proteins associated, as is the case, for example, with Ad5E1B55K and p53 (57). To
254 examine this possibility, initially GST pull-down assays were carried out with purified GST-Tab182 (C-
255 terminal region) and whole cell lysates from E1B55K-expressing Ad12E1HER2 and Ad5E1HEK293
256 cells. In both cases the E1B55K protein was identified as a binding partner (Figures 9A and 9B). As

257 well as GST, GST-PRMT1 was included as an irrelevant (negative) control as it is of comparable
258 molecular weight to the Tab182 polypeptide. No binding of GST or GST-PRMT1 to E1B55K proteins
259 was seen. In further experiments, using the same cell lines, E1B55K proteins were co-
260 immunoprecipitated using an antibody against Tab182 (Figures 9C and 9D). No co-
261 immunoprecipitation was seen using an irrelevant antibody against collagen IV. In a further
262 experiment, Ad5E1HEK293 cells and Ad12E1HER2 cells were transfected with a construct encoding
263 GFP-Tab182. The lysates were immunoprecipitated with antibodies against AdE1B55K proteins and
264 co-precipitated Tab182 detected by western blotting (Figure 9E). The slightly higher molecular
265 weight GFP-Tab182 and the endogenous Tab182 were both seen in some lanes. These results
266 strongly suggest that, in both Ad5 and Ad12 serotypes, the viral E1B55K proteins interact directly
267 with Tab182.
268 Although degradation of Tab182 occurs to only a very limited extent during infection with
269 adenoviruses other than Ad5 and Ad12 (Figure 5) we considered the possibility that the E1B55K
270 proteins from these other species may also associate with Tab182. Therefore, HeLa cells were
271 transfected with constructs encoding HA-tagged Ad9E1B55K (group D) or HA-tagged Ad16E1B55K
272 (group B1). After 48 hours Tab182 was immunoprecipitated and associated E1B55K protein detected
273 with an antibody against HA (Figure 9F). It can be seen that whilst the Ad9 protein bound strongly
274 the Ad16 equivalent could only be seen on over-exposed western blots, indicating a very weak
275 association (Figure 9G). Similar results were obtained when the constructs were transfected into
276 Ad5E1HEK293 cells (data not shown). To check whether this differentiation extends to other
277 adenovirus targets the interaction with p53 was examined. After transfection of both constructs into
278 Ad5E1HEK293 cells, HA-tagged E1B55K proteins were immunoprecipitated and bound p53 detected
279 by western blotting (Figure 9H). In contrast to Tab182, both Ad9 and Ad16E1B55K proteins strongly
280 interacted with p53.
281 It is now well-established that the small DNA tumour viruses have many cellular targets in common,
282 such as pRb, p53 and CBP/p300 (58 and 59). It has already been reported that the E6 protein from

283 HPV genus beta, species 2 (HPV17a and HPV38) associates with the CNOT complex (60). To examine
284 if Tab182 interacts with proteins from other small DNA tumour viruses, a co-immunoprecipitation
285 experiment was carried out with Tab182 antibody using 293FT cells which express SV40 T antigen.
286 When Tab182 was immunoprecipitated appreciable SV40T was associated with it (Figure 9I).

287 *Tab182 is a component of the CNOT complex.*

288 It has previously been noted that Tab182 can be co-immunoprecipitated with the CNOT complex
289 from mammalian cells (40). To confirm this association, Tab182 was immunoprecipitated, using the
290 rabbit antibody raised against the C-terminal fragment, and the total immunoprecipitate analysed by
291 mass spectrometry. Results from a representative co-immunoprecipitation experiment are
292 presented in Table 1. In all cases most components of the CNOT complex were detected although
293 there were limited variations from one experiment to the next. Specifically, CNOT4 was never
294 detected in any Tab182 co-immunoprecipitate and CNOT 7 and CNOT 8 were occasionally not
295 identified. Significantly, neither Tab182 nor CNOT proteins were detected in any of the control
296 immunoprecipitates carried out with rabbit IgG (data not shown). Proteins which were seen in both
297 Tab182 and control IgG immunoprecipitations have not been listed in Table 1. The proteins listed are
298 the only ones which were consistently observed in five Tab182 immunoprecipitation experiments
299 but not in controls.

300 In a final set of co-immunoprecipitations we investigated whether AdE1B55K proteins were
301 associated with other CNOT components. Using the adenovirus E1-expressing cells, CNOT1 was
302 immunoprecipitated and associated E1B55K proteins detected by Western blotting (Figures 9J and
303 9K). It is possible that these results show direct interaction of the viral proteins with CNOT1 but
304 could also indicate interaction with other, as yet unidentified, components of the intact CNOT
305 complex or even Tab182.

306 *Adenovirus infection leads to a reduction in the levels of other CNOT proteins*

307 In light of the co-immunoprecipitation experiments shown in Table 1 and Figure 9 we examined the
308 levels of other CNOT proteins during adenovirus infection. Following infection of HeLa cells with

either Ad5 or Ad12 levels of CNOT1, CNOT3, CNOT4 and CNOT7 were monitored by Western blotting (Figure 10) In contrast to Tab182, levels of CNOT1 and CNOT4 remained stable throughout the time course of infection (Figures 10A and 10B). However, levels of both CNOT3 and CNOT7 were markedly reduced after infection with both serotypes. In the case of Ad5, levels of CNOT3 decline prior to the observed decrease in CNOT7 whereas for Ad12 CNOT7 levels decline prior to CNOT3 (Figures10A and 10B). Further work will be required to determine whether these proteins are degraded in the same fashion as Tab182 and whether levels of other CNOT proteins are reduced during adenovirus infection but these data suggest that the complex may be a major target for certain adenoviruses.

Tab182 and CNOT1 depletion favours adenovirus infection

To determine what advantage adenoviruses might derive from the degradation of Tab182 and other CNOT complex proteins, a time course of infection was followed in HeLa cells treated with Tab182 siRNA. In addition, the effect of depletion of CNOT1 was also examined. CNOT1 forms a scaffold on which other members of the complex associate (41). We, therefore, reasoned that its depletion would cause maximal disruption of CNOT complex activity. Cells were infected with Ad5 and Ad12 48 hours after the addition of control, Tab182 or CNOT1 siRNAs. It can be seen from Figures 11A and 11B that, in the absence of Tab182, expression levels of the E1A viral proteins were elevated to a limited extent compared to controls, during the time-course of infection. Similar results were obtained with the E1B55K negative viruses, Ad5*dl*1520 and Ad12*dl*620, in that AdE1A proteins were expressed at a higher level in the absence of Tab182 (data not shown). In the samples treated with control siRNA there is a reduction in the level of Tab182 as degradation proceeds. Expression of other viral proteins varied marginally between Tab182-depleted and control cells. However, in a further set of experiments it was shown that when CNOT1 was depleted before infection with Ad5 there was a notable increase in E1A and E1B55K expression compared to controls (Figure 11A). In Ad12 infected cells there was an even more marked increase in expression of the E1A and E1B55K proteins, compared to control siRNA treated cells (Figure 11B). From the western blots it is clear

that Tab182 depletion has its most marked effect at 24 hours post Ad12 infection. However, depletion of CNOT1 causes a several fold increase in Ad12E1A expression at 24 hours but, notably, the level of protein stays consistently high up to 96 hours. The effects on Ad5E1A were less pronounced, although, again, loss of Tab182 had most effect at 24 hours post infection whereas depletion of CNOT1 facilitated AdE1A expression up to 96 hours.

It has long been known that adenovirus infection promotes cell cycle progression from G1 into a 'psuedo S-phase' accompanied by enhanced expression of cyclin E (reviewed in 61, for example). In addition, it has also been reported that Ad E1A promotes expression of the tyrosine phosphatase CDC25A, which is required for the G1 to S-phase transition (62). In an attempt to examine whether the depletion of Tab182 and CNOT1 affects the ability of adenoviruses to initiate cell cycle progression the expression of CDC25A was initially examined. It is notable that, in the Tab182 and CNOT1 depleted cells, there is only very limited induction of CDC25A after infection whereas this is appreciable in the control infected cells (Figure 11A and 11B). After 24 hours in all cases, expression returns to a low level comparable with uninfected cells. We suggest that low level expression of CDC25A is required by the virus for progression of the infected cells into pseudo S-phase but after that, to stop further progression, CDC25A may be detrimental to viral replication. It is possible that reduction in CNOT components decreases CDC25A, retaining the cells in a cell cycle phase more conducive to viral early protein expression and viral replication.

Tab182 depletion favours progression into S phase after adenovirus infection

In view of the CDC25A western blotting data shown in Figure 11, the effects of depletion of Tab182 or CNOT1 on cyclin E expression were also examined. HeLa cells were again treated with control, Tab182 and CNOT1 siRNAs, mock-infected or infected with Ad12 and then harvested at various times up to 96 hours. In the mock-infected cells treated with control siRNA cyclin E is expressed at constant low level but in those cells treated with Tab182 and particularly CNOT1 siRNAs there is an appreciable elevation in cyclin E expression (Figure 12A). When a similar set of cells were infected with Ad12 elevated cyclin E levels were also observed (Figure 12B). Thus, in control infected cells

there was a limited increase in cyclin E expression but in the absence of Tab182 or CNOT1, expression of cyclin E is elevated to a much greater extent (Figure 12B). It seems likely, therefore, that effects seen in the virally infected cells are primarily attributable to CNOT1 and Tab182 depletion rather than the virus itself. The advantage gained by the virus, facilitating E1A expression, could be due to the fact that the siRNA treated cells have generally progressed slightly further through the cell cycle, into a phase more favourable for adenovirus early protein expression, as suggested in the previous section. Ad5 infection of HeLa cells treated with the same siRNAs had little additional effect on cyclin E expression (data not shown).

Tab182 and CNOT1 depletion enhances the AdE1A mRNA expression

To determine whether depletion of Tab182 or CNOT1 affects AdE1A expression at the transcriptional level, cells depleted of either Tab182 or CNOT1 were infected with either Ad5 or Ad12 before isolation of total RNA after 24 hours. RT-PCR was performed following reverse transcription of total RNA to amplify Ad5 and Ad12 13S E1As using primers across the CR3 unique region of each protein; Ct values were calculated, normalised to GAPDH. Depletion of CNOT1 or Tab182 in Ad5 or Ad12 infected cells was verified by western blotting (data not shown). The relative expression of 13S E1A in infected cells with depleted CNOT1 or Tab182 was compared with mock-transfected, infected cells. It can be seen from the data presented in Figure 13 that depletion of Tab182 resulted in an increase in both Ad5 and Ad12 13S E1A mRNAs compared to controls. The depletion of CNOT1 had a more marked effect, consistent with the western blots shown in Figure 11.

Tab182 and CNOT1 depletion favours the production of viral DNA during infection

To examine whether the advantage gained in the expression of early proteins in Tab182 and CNOT1 depleted cells extends to the production of viral genomes HeLa cells were treated with appropriate siRNAs and infected with Ad5 and Ad12 48 hours later. After a further 24 hours cells were harvested and the DNA isolated. The concentration of adenovirus DNA was measured by quantitative PCR as outlined in the Materials and Methods using primers equivalent to Hexon and GAPDH as a control. More viral DNA can be seen in the Tab182 depleted cells than in the control cells after both Ad5 and

Ad12 infection (Figure 14); similarly, there is an even greater increase after CNOT1 depletion, consistent with increased AdE1A expression. Interestingly, the effect of CNOT1 and Tab182 depletion were very similar during Ad5 infection (Figure 14A) whereas CNOT1 depletion had an appreciably greater effect than Tab182 depletion in Ad12 infected cells (Figure 14B).

Discussion

It is now well-established that adenovirus infection triggers a cellular DDR (22). This is counteracted, in Ad5 and Ad12 at least, by the degradation of multiple cellular proteins. Initially, it was noted that p53 was a target for proteasome-mediated degradation during adenovirus infection (63 and 64). This has been followed by demonstrations that other DDR proteins, such as MRE11, BLM and DNA Ligase IV, are targeted to the proteasome through the actions of the viral E1B55K and E4orf6 proteins (10, 11 and 24). Whilst this is the case for the group A and group C viruses it certainly does not apply universally to all adenovirus serotypes (28 and 56). In particular, it has been shown that group B (for example, Ad7, Ad11 and Ad16) and group D (for example, Ad9) viruses target a much more limited set of DDR proteins, possibly not extending beyond DNA Ligase IV. Furthermore, it seems that the E1B55K/E4orf6 complex is not always required as degradation of TOPBP1 requires only Ad12E4orf6, whereas DAXX degradation utilizes only Ad5E1B55K (12 and 27).

In a screen looking for additional DNA damage response proteins which might be targeted for adenovirus-mediated degradation we have identified Tab182 and, subsequently other members of the CNOT complex, CNOT7 and CNOT3, as probable targets. Tab182 was originally shown to interact with tankyrase 1 (32) and to be highly phosphorylated by ATM and/or ATR after DNA damage by IR (33). More recently, evidence has been presented to show that Tab182 plays a role in DSB repair and promotes the association of PARP-1 with the DNA-PK catalytic subunit (34, 35).

There had been suggestions that Tab182 was a peripheral component of the CNOT complex in mammals (40) and it was identified in various complexes in large scale protein interactome screens (see, for example, 65-67). We have now confirmed that Tab182 is an integral component of the

413 CNOT complex. Depletion of the protein increases the sensitivity of cells to damage induced by
414 ionising radiation, UV radiation and HU and impairs the cell's ability to form DNA repair foci
415 following DNA replication stress (34, 35 and our unpublished data).
416 Here it has been shown that Tab182 is degraded during Ad5 and Ad12 infection (Figure 1). In both
417 cases this requires the AdE1B55K and AdE4orf6 proteins but is independent of AdE4orf3 which has
418 been shown to be required for degradation of other cellular proteins (25) (Figures 1 and 2).
419 Degradation of Tab182 is inhibited by bortezomib, a proteasome inhibitor, and MLN4924, which
420 inhibits cullin NEDDylation, preventing its activation (Figures 6 and 7). As is the case for p53
421 degradation, Ad12 hi-jacks a cullin 2-based E3 ligase (Figure 7), although it appears that ablation of
422 either Cul2 or Cul5 expression has a similar effect on Tab182 degradation during Ad5 infection
423 (Figure 7) in that loss of either causes partial protein stabilization. Clarification of this observation
424 requires further investigation.
425 To confirm the results of the mutant virus infections, that Tab182 is targeted through AdE1B55K, co-
426 immunoprecipitation assays were carried out and it was found that Tab182 and both the Ad5 and
427 Ad12 proteins could be immunoprecipitated together. Furthermore, both Ad5 and Ad12 E1B55K
428 proteins bound to the GST-Tab182 C-terminal region, indicating a direct interaction (Figure 9).
429 Interestingly, Tab182 binds strongly to Ad9E1B55K but not Ad16E1B55K although it does not appear
430 to be degraded by either group B1 (Ad7 and Ad16) or group D (Ad9) viruses (Figures 5 and 9).
431 E1B55K proteins from both Ad9 and Ad16 interact with p53 as might be expected since it is
432 transcriptionally inactive after Ad9 and Ad7 infection, even though it is present at high level (28).
433 These observations suggest that interaction of E1B55K with Tab182 may be determined by factors
434 other than a requirement for protein degradation. A more widespread examination of the
435 interaction of Tab182 with E1B55K proteins from a number of adenoviruses may elucidate this point.
436 Tab182 also associates with SV40T antigen in co-immunoprecipitation experiments, suggesting that
437 the protein could be a target for the family of small DNA tumour viruses (Figure 9I). Significantly,

438 previous studies have shown that the CNOT complex associates with HPV17a and HPV38 E6 proteins
439 although the consequences of this for the virus were not examined at the time (60).
440 To see how extensive the relationship between adenoviruses and the CNOT complex was, the fate of
441 other components of the complex was studied following adenovirus infection (Figure 10). Although
442 only a limited number of CNOT proteins were examined it was seen that levels of CNOT3 and CNOT7
443 were reduced during Ad5 and Ad12 infection whereas levels of CNOT4 and CNOT1 remained stable.
444 Although a number of activities have been attributed to the CNOT complex, such as deadenylase,
445 transcriptional regulation and ubiquitin E3 ligase activity (37-39 and 46-48) it is not clear what
446 contribution Tab182 makes. To attempt to understand why adenovirus might target Tab182 (and
447 other CNOT proteins) adenovirus infection was compared in control and siRNA knock down cells. It
448 was seen that expression of E1A was enhanced, to a limited extent, in Tab182 depleted cells
449 although little or no difference was seen in the expression of late proteins (Figure 11). To see if a
450 similar effect occurred with other members of the CNOT complex, CNOT1, which is considered to be
451 a scaffold protein required for the integrity of the complex, was depleted. During Ad5 infection E1A
452 expression was notably increased when CNOT1 was depleted while in the case of Ad12 there was a
453 greatly enhanced expression of E1A and a marked increase in E1B55K protein, following CNOT1
454 knock down, compared to controls (Figure 11). The increased effect of CNOT1 protein depletion on
455 Ad12 compared to Ad5 appears to be consistent with Ad12's somewhat enhanced ability to degrade
456 Tab182. The difference in expression of E1A protein is due to an increase in AdE1A mRNA, as shown
457 by RT-PCR (Figure 13). Whether this effect is directly attributable to a reduction in deadenylase
458 activity of the CNOT complex will have to await further investigation. Interestingly, it has recently
459 been shown that the Ad5 E1B55K/E4orf6 complex enhances E1A activity by stabilizing the protein,
460 leading to increased level, and by increasing the activation of E2F by E1A (68). It is possible that the
461 effect of the same adenovirus complex on the CNOT complex, as demonstrated here, could
462 contribute to the increased AdE1A level observed. In a further study it has been shown that the
463 concentration of viral DNA is increased in Tab182 and CNOT1 depleted cells 24 hours after both Ad5

464 and Ad12 infection (Figure 14). More marked effects were seen with CNOT1 depletion than with
465 Tab182 consistent with the observed increase in AdE1A expression (Figure 11); however, reduction
466 in Tab182 had less effect on relative Hexon DNA concentration after Ad12 infection than with Ad5,
467 reasons for this are not clear at present.
468 The relationship between adenoviruses and the CNOT complex is not clear cut, for whilst the virus is
469 able to cause degradation of various components this occurs later than any initial enhanced increase
470 in AdE1A expression seen after the depletion of CNOT proteins described here. It is notable that
471 there is a sustained increase in AdE1A expression up to 96 hours in the absence of CNOT1 (Figure
472 11). However, increases in viral DNA concentration were observed after CNOT1 and Tab182
473 depletion, suggesting that inactivation of the complex will facilitate viral replication to a limited
474 extent. It is also possible that the aim of the virus, in degrading and presumably inactivating the
475 CNOT complex, is not necessarily just to facilitate AdE1A expression, but to fulfil some other, as yet
476 unidentified, role, perhaps linked to an effect on the DDR. It should be borne in mind, when
477 considering the effects of CNOT1 depletion, that adenoviruses do not actually cause its degradation
478 and while its loss will probably indicate the effect of inactivation of the CNOT complex it does not
479 necessarily coincide with what happens *in vivo*. It is also possible that other CNOT proteins could be
480 targets for adenovirus-mediated degradation early in infection co-incident with AdE1A expression,
481 although we have no evidence of this. Significantly, degradation of Tab182 and CNOT7 occurs later in
482 viral infection than is the case for MRE11 and BLM and is more similar to that seen for p53.
483 Loss of components of the CNOT complex, for example Tab182, appears to facilitate progression of
484 cells into late G1/early S-phase, as evidenced by the enhanced expression of cyclin E and transitorily
485 enhanced expression of CDC25A (Figures 11 and 12). This may provide an environment more
486 conducive to expression of early viral proteins, particularly E1A. For reasons which are not evident at
487 present the effect seems to be more marked with Ad12 compared to Ad5. With relevance to the
488 effects on cyclin E expression, it is worth noting that CNOT1 depletion has a more marked effect

than does Tab182 depletion, suggesting that its loss enhances cell cycle progression to a greater extent. However, it is possible that loss of other CNOT proteins could have a comparable effect.

In summary, Ad5 and, in particular, Ad12 have been shown to target Tab182 and other CNOT proteins for proteasome-mediated degradation during viral infection. Loss of Tab182 and CNOT1 favours enhanced expression of AdE1A and E1B55K proteins in the early stages of infection.

Materials and methods

Cell lines, viruses and plasmids.

HeLa (obtained from ATCC), HEK293FT (Invitrogen), Ad5E1HEK293 (a generous gift from Frank Graham), and Ad12E1HER2 (69) cells were grown in DMEM supplemented with 8% foetal calf serum (FCS). H1299-based cell lines in which Cul2 or Cul5 expression had been ablated were a generous gift from Paola Blanchette and Phil Branton. The cells were grown in DMEM supplemented with 8% FCS and 1 µg/ml puromycin (Cul2$^-$) or 8 % FCS, 1 µg/ml puromycin and 100 µg/ml hygromycin (Cul5$^-$). Ad4, Ad5, Ad7, Ad9, Ad11 and Ad12 viruses were obtained from ATCC or were a generous gift from Jo Mymryk. The following Ad5 mutant viruses were used: Ad5*dl*1520 (Ad5E1B55K$^-$) (70), H5*in*351 (E4orf1$^-$), H5*pm*4154 (E4orf6$^-$), H5*pm*4155 (E4orf3$^-$, E4orf6$^-$), H5*pm*4166 (E4orf4$^-$), H5*dl*356 (E4orf7$^-$) and H5*in*352 (E4orf2$^-$) (23, 26, 71-73). In addition, an Ad12 E1B55K negative mutant virus (Ad12*dl*620) was used (74). HeLa cells were generally infected at a multiplicity of infection of 5 plaque forming units (pfu)/cell. Ad5 and Ad12 E1B55K DNA was cloned into pcDNA3 and Ad5 and Ad12 E4orf6-HA tag DNA was also cloned into pcDNA3 as previous described (75). NEDDylation was inhibited by addition of MLN4924 to the cell culture medium at a concentration of 4 µM and proteasomal activity was inhibited with bortezomib (0.5 µM).

siRNA treatment to deplete Tab182 and CNOT proteins and protein transfections.

HeLa cells were plated at a density of $4x10^5$ per 6 cm dish. After 24 hours they were transfected with control or ON-TARGETplus SMART pool siRNAs (0.2 nmol/dish) (GE Dharmacon) directed against Tab182 or CNOT1 proteins using Oligofectamine (Invitrogen) following the manufacturer's protocol. After 24hours cells were split 1→3 and after a further 24hours infected with virus. For protein

transfections cells were grown to 70% confluency and then incubated with DNA constructs (2µg/6cm dish or 5µg/10cm dish) which had been previously mixed for 20 minutes with Lipofectamine 2000 (Invitrogen) in Opti-Mem (Gibco) following the manufacturer's protocol. After 24 hours cells were incubated with fresh medium and harvested 24 hours later.

Cloning Tab182

Total cellular RNA was isolated from a lymphoblastoid cell line from a normal individual using the Qiagen RNeasy Mini Kit and was reverse transcribed into cDNA using the oligo-dT primer d(T)23VN and the Protoscript II First Strand cDNA Synthesis Kit (New England Biolabs). PCR was used to amplify the complete Tab182 cDNA sequence using the forward primer (For 1) 5'-GAGCGGGTCGAC*GATG*AAAGTGTCTACTCTCAGG-3' and the reverse primer (Rev13) 5'-CGTGATGTCGAC*TCA*GACCTTCTTCTTCTTCAGTTT-3'. Both primers contain the recognition sequence for the restriction enzyme *Sal* I (underlined). The forward primer contains the translation initiation codon for Tab182 (italics) and the reverse primer contains the translation termination codon for Tab182 (italics; strand antiparallel to sense strand). The Tab182 cDNA sequence was amplified using Q5 High-Fidelity DNA Polymerase (New England Biolabs). An initial denaturation step of 98ºC for 30 seconds was followed by 30 cycles of 98ºC for 5 seconds, 62ºC for 15 seconds and 72ºC for 4 minutes. A final extension of 5 minutes at 72ºC followed the 30 cycles. The PCR products were analysed by gel electrophoresis and a product of the correct size (5190 base pairs) was identified. The products were digested with *Sal* I-HF and the excised Tab182 band purified by gel electrophoresis. Tab182 was cloned into the pEGFP-C3 plasmid. Sequence determination was performed using an Applied Biosystems 3500xL Genetic Analyzer. Sequences were analysed on-line using BLAST at the National Center for Biotechnology Information (NCBI). Sequences were all wild type. Codon 322 can encode threonine (ACT) or serine (AGT) and the ratio is approximately equal in the general population. The sequences isolated from the individual used to make the cDNA for this cloning exercise were all found to encode serine at amino acid 322.

Isolation of RNA and cDNA Synthesis

Cellular RNA was extracted using the SV Total RNA Isolation System (Promega) following the manufacturer's protocol. To remove any DNA contamination, RNA was treated with DNase I (Promega). RNA quantity and quality were evaluated by optical density measurements (260/280 nm ratios) and by agarose gel electrophoresis. First-strand cDNA synthesis was performed using SuperScript™ II Reverse Transcriptase (RT) (Invitrogen) and random primers according to the manufacturer's instructions.

Isolation of genomic DNA

Cellular DNA was extracted using the QIAamp DNA Mini Kit (Qiagen) following the manufacturer's protocol. In order to remove any protein or RNA contamination 15 µl Proteinase K (10 mg/ ml) (Sigma-Aldrich) and 4 µl RNase A (20 mg/ml) (Invitrogen) were added to each sample. DNA quantity and quality were evaluated by optical density measurements (260/280 nm ratios) and by agarose gel electrophoresis.

Primer design and RT-PCR

Cellular RNA or DNA was extracted as described above. The sequences of the primers used for RT-PCR are as shown in Table 2. Specificity of the primers was checked with NCBI/Primer-BLAST.

The RT-PCR reactions were performed in the Mx3005P system (Stratagene) using real-time PowerUp™ SYBR® Green Master Mix (Applied Biosystems). Quantitative RT-PCR was carried out in a final volume of 20 µl containing 2 µg or 10ng of cDNA or DNA, respectively, 5 pmol of the forward primer, 5 pmol reverse-primer and 10 µl of PowerUp™ SYBR® Green Master Mix. Thermocycling program was performed for 10 min at 95ºC for the pre-cycling step to denature the cDNA and to activate Dual-Lock™ Taq DNA Polymerase, and then followed by 35 cycles of denaturation at 95ºC for 30 sec, annealing at 55ºC for 1 min and extension at 72ºC for 1 min. To confirm the expected amplifications 2% agarose gel electrophoresis with ethidium bromide staining was performed. Viral AdE1A or Hexon and host cell Tab182 and CNOT1 Ct values were normalized to Ct values of GAPDH

amplified from the same sample [for example, ΔCt = Ct (Tab182) − Ct (GAPDH)], and the 2−ΔΔCt method was used to calculate the relative-expression. Each experiment was performed in triplicate.

Western blotting and antibodies.

Cells were harvested after washing with ice-cold phosphate buffered saline (PBS) and solubilised in 8 M urea, 50 mM Tris HCl pH7.4, and 0.15 M β-mercaptoethanol. Proteins were fractionated on polyacrylamide gels in the presence of 0.1 M Tris, 0.1 M Bicine, and 0.1% SDS. For western blotting, proteins were electrophoretically transferred to nitrocellulose membranes before incubation with antibodies overnight at 4^{o}C. Antibodies used in the study were as follows: Tab182 (an antibody raised in rabbits against GST-Tab182 [C-terminal fragment]), MRE11, CNOT3, CNOT4, CNOT7, (all from GeneTex), CNOT1 (Proteintech), cullin2, cyclin E1, RPA32 (Abcam), p53 (raised in rabbits), cullin5, GAPDH, collagen IV, SV40T (Santa Cruz Biotechnology), and β actin (Sigma-Aldrich). Rabbit antibodies against Ad5 Hexon and Ad12 Fiber protein were gifts from Vivien Mautner and Paul Freimuth, respectively. A mouse monoclonal antibody against Ad5DNA binding protein (DBP) was a gift from Pieter van der Vliet. Antibodies against Ad5E1A (M73), Ad12E1A (5DO2), Ad12E1B55K (XPH9), Ad5E1B55K (2A6), p53 (DO1) and HA (12CA5) were purified from monoclonal supernatants.

GST pull-down assays and co-immunoprecipitation

The C-terminal fragment of Tab182 (amino acids 824-867+1221-1729) was expressed in *E.coli* as a GST fusion protein as described (49). For GST pull-down and co-immunoprecipitation assays cells were harvested in ice-cold PBS and lysed in 0.4 M NaCl, 40 mM Tris HCl pH7.4, 5 mM EDTA, 1% NP40. Insoluble protein was removed by centrifugation (45K, 30 minutes, 4^{o}C). Lysates were incubated overnight either with GST fusion protein or appropriate antibody. Protein complexes were retrieved on glutathione-agarose beads or Protein G-agarose beads as appropriate. After washing with lysis buffer, bound proteins were released with either 25mM glutathione, pH8.2 (GST fusion proteins) or SDS sample buffer (immunoprecipitated samples) and fractionated by SDS-PAGE prior to western blotting.

Mass spectrometry

591 Proteins were immunoprecipitated as described above except that the antibody-antigen complexes
592 were released with 8 M urea, 50 mM NH_4HCO_3 for 30 minutes at ambient temperature. Proteins
593 were reduced in 50 mM DTT, 50 mM NH_4HCO_3 at 56^{o}C for 30 minutes and then carboxymethylated
594 in 100 mM iodoacetamide at ambient temperature in the dark for 30 minutes. Proteins were
595 retrieved using Amicon centrifugal filters (30K molecular weight cut off) which were washed four
596 times with 50 mM NH_4HCO_3. The filters, with the bound immunoprecipitated proteins, were
597 incubated overnight at 37^{o}C with trypsin (1 µg) in 50 mM NH_4HCO_3. Tryptic peptides were retrieved
598 by centrifugation, dried and analysed using a Bruker amaZon ion trap mass spectrometer. Peptides
599 were identified using the ProteinScape central bioinformatics platform (Bruker).
600 *Immunofluorescence microscopy*
601 HeLa cells were grown on glass cover slips. After 24 hours cells were infected or mock infected with
602 Ad5 or Ad12 (5pfu/cell) for 30 hours. Cells were fixed in 3.6% para-formaldehyde in PBS for 10
603 minutes and permeabilized in 0.5% TritonX-100 in PBS for 5 minutes. Fixed cells were stained with
604 primary antibodies for 1 hour, washed three times in PBS and stained with secondary antibodies also
605 for 1 hour. DNA was stained with DAPI. When pre-extraction was used cells were treated with pre-
606 extraction buffer (10 mM PIPES, 20 mM NaCl, 3 mM MgCl2, 300 mM sucrose, 0.5% Triton X-100) for
607 7 minutes on ice before fixing with 3.6% para-formaldehyde and antibody staining as above.
608 Fluorescence images were taken using a Nikon E600 Eclipse microscope333 equipped with a 60X oil
609 lens, and images were acquired and analysed using Volocity Software 334 v4.1 (Improvision).
610

611 **Acknowledgments**
612 We are most grateful to Martin Higgs, Natasha Zlatanou, John Reynolds and Joanna Parish for
613 helpful discussion. We also thank Susan Smith, Clare Davies, Phil Branton and Paola Blanchette for
614 gifts of reagents. We thank The Medical Research Council (MRC), through the University of
615 Birmingham, and Cancer Research UK (CRUK) for funding. We also thank Katie Grand for charitable
616 donations.

617 **References**

618 1 Berk AJ. Adenoviridae: the viruses and their replication, in: K.D. Fields B.N, P.M. Howley, et al.
619 (Eds.), Virology, 5th edn., Lippincott Williams & Wilkins, Philadelphia, 2007, pp. 2355–2394

620 2 Berk AJ. Recent lessons in gene expression, cell cycle control, and cell biology from adenovirus.
621 Oncogene. 2005; 24(52):7673-85.

622 3 Gallimore PH, Turnell AS. Adenovirus E1A: remodelling the host cell, a life or death experience.
623 Oncogene. 2001; 20(54):7824-35.

624 4 Pelka P, Ablack JN, Fonseca GJ, Yousef AF, Mymryk JS. Intrinsic structural disorder in adenovirus
625 E1A: a viral molecular hub linking multiple diverse processes. J Virol. 2008; 82(15):7252-63.

626 5 Endter C, Dobner T. Cell transformation by human adenoviruses. Curr Top Microbiol Immunol.
627 2004 273: 163-214.

628 6 Carson CT, Schwartz RA, Stracker TH, Lilley CE, Lee DV, Weitzman MD. The MRE11 complex is
629 required for ATM activation and the G2/M checkpoint. EMBO J. 2003; 22(24):6610-20.

630 7 Carson CT, Orazio NI, Lee DV, Suh J, Bekker-Jensen S, Araujo FD, Lakdawala SS, Lilley CE, Bartek J,
631 Lukas J, Weitzman MD. Mislocalization of the MRN complex prevents ATR signaling during
632 adenovirus infection. EMBO J. 2009; 28(6):652-62.

633 8 Blackford AN, Bruton RK, Dirlik O, Stewart GS, Taylor AM, Dobner T, Grand RJ, Turnell AS. A role for
634 E1B-AP5 in ATR signaling pathways during adenovirus infection. J Virol. 2008; 82(15):7640-52.

635 9 Querido E, Blanchette P, Yan Q, Kamura T, Morrison M, Boivin D, Kaelin WG, Conaway RC,
636 Conaway JW, Branton PE. Degradation of p53 by adenovirus E4orf6 and E1B55K proteins occurs via a
637 novel mechanism involving a Cullin-containing complex. Genes Dev. 2001; 15(23):3104-17.

638 10 Stracker TH, Carson CT, Weitzman MD. Adenovirus oncoproteins inactivate the MRE11-Rad50-
639 NBS1 DNA repair complex. Nature. 2002; 418(6895):348-52.

640 11 Baker A, Rohleder KJ, Hanakahi LA, Ketner G. Adenovirus E4 34k and E1b 55k oncoproteins target
641 host DNA ligase IV for proteasomal degradation. J Virol. 2007; 81(13):7034-40.

642 12 Blackford AN, Patel RN, Forrester NA, Theil K, Groitl P, Stewart GS, Taylor AM, Morgan IM, Dobner
643 T, Grand RJ, Turnell AS. Adenovirus 12 E4orf6 inhibits ATR activation by promoting TOPBP1
644 degradation. Proc Natl Acad Sci U S A. 2010; 107(27):12251-6
645 13 Ciccia A, Elledge SJ. The DNA damage response: making it safe to play with knives. Mol Cell. 2010;
646 40(2):179-204.
647 14 Jackson SP, Bartek J. The DNA-damage response in human biology and disease. Nature. 2009;
648 461(7267):1071-8.
649 15 Lukas J, Lukas C, Bartek J. More than just a focus: The chromatin response to DNA damage and its
650 role in genome integrity maintenance. Nat Cell Biol. 2011; 13(10):1161-9.
651 16 Bhatti S, Kozlov S, Farooqi AA, Naqi A, Lavin M, Khanna KK. ATM protein kinase: the linchpin of
652 cellular defenses to stress. Cell Mol Life Sci. 2011; 68(18):2977-3006.
653 17 Blackford AN, Jackson SP. ATM, ATR, and DNA-PK: The Trinity at the Heart of the DNA Damage
654 Response. Mol Cell. 2017; 66(6):801-817.
655 18 Cimprich KA, Cortez D. ATR: an essential regulator of genome integrity. Nat Rev Mol Cell Biol.
656 2008; 9(8):616-27.
657 19 Nam EA, Cortez D. ATR signalling: more than meeting at the fork. Biochem J. 2011; 436(3):527-36.
658 20 Weiden MD, Ginsberg HS. Deletion of the E4 region of the genome produces adenovirus DNA
659 concatemers. Proc Natl Acad Sci U S A. 1994; 91(1):153-7.
660 21 Blackford AN, Grand RJ. Adenovirus E1B 55-kilodalton protein: multiple roles in viral infection
661 and cell transformation. J Virol. 2009; 83(9):4000-12.
662 22 Turnell AS, Grand RJ. DNA viruses and the cellular DNA-damage response. J Gen Virol. 2012; 93(Pt
663 10):2076-97.
664 23 Schreiner S, Wimmer P, Dobner T. Adenovirus degradation of cellular proteins. Future Microbiol.
665 2012; 7(2):211-225.
666 24 Orazio NI, Naeger CM, Karlseder J, Weitzman MD. The adenovirus E1b55K/E4orf6 complex
667 induces degradation of the Bloom helicase during infection. J Virol. 2011; 85(4):1887-92.

668 25 Forrester NA, Patel RN, Speiseder T, Groitl P, Sedgwick GG, Shimwell NJ, Seed RI, Catnaigh PÓ,
669 McCabe CJ, Stewart GS, Dobner T, Grand RJ, Martin A, Turnell AS. Adenovirus E4orf3 targets
670 transcriptional intermediary factor 1γ for proteasome-dependent degradation during infection. J
671 Virol. 2012; 86(6):3167-79.
672 26 Dallaire F, Blanchette P, Groitl P, Dobner T, Branton PE. Identification of integrin alpha3 as a new
673 substrate of the adenovirus E4orf6/E1B 55-kilodalton E3 ubiquitin ligase complex. J Virol. 2009;
674 83(11):5329-38.
675 27 Schreiner S, Wimmer P, Groitl P, Chen SY, Blanchette P, Branton PE, Dobner T. Adenovirus type 5
676 early region 1B 55K oncoprotein-dependent degradation of cellular factor Daxx is required for
677 efficient transformation of primary rodent cells. J Virol. 2011; 85(17):8752-65.
678 28 Forrester NA, Sedgwick GG, Thomas A, Blackford AN, Speiseder T, Dobner T, Byrd PJ, Stewart GS,
679 Turnell AS, Grand RJ. Serotype-specific inactivation of the cellular DNA damage response during
680 adenovirus infection. J Virol. 2011; 85(5):2201-11.
681 29 Araujo FD, Stracker TH, Carson CT, Lee DV, Weitzman MD. Adenovirus type 5 E4orf3 protein
682 targets the MRE11 complex to cytoplasmic aggresomes. J Virol. 2005; 79(17):11382-91.
683 30 Blanchette P, Wimmer P, Dallaire F, Cheng CY, Branton PE. Aggresome formation by the
684 adenoviral protein E1B55K is not conserved among adenovirus species and is not required for
685 efficient degradation of nuclear substrates. J Virol. 2013; 87(9):4872-81.
686 31 Liu Y, Shevchenko A, Shevchenko A, Berk AJ. Adenovirus exploits the cellular aggresome response
687 to accelerate inactivation of the MRN complex J Virol. 2005; 79(22):14004-16.
688 32 Seimiya H, Smith S. The telomeric poly (ADP-ribose) polymerase, tankyrase 1, contains multiple
689 binding sites for telomeric repeat binding factor 1 (TRF1) and a novel acceptor, 182-kDa tankyrase-
690 binding protein (TAB182). J Biol Chem. 2002; 277(16):14116-26.
691 33 Matsuoka S, Ballif BA, Smogorzewska A, McDonald ER 3rd, Hurov KE, Luo J, Bakalarski CE, Zhao Z,
692 Solimini N, Lerenthal Y, Shiloh Y, Gygi SP, Elledge SJ. ATM and ATR substrate analysis reveals
693 extensive protein networks responsive to DNA damage. Science. 2007; 316(5828):1160-6.

694 34 Zou L-H, Shang Z-F, Tan W, Liu X-D, Xu Q-Z, Song M, Wang Y, Guan H, Zhang S-M, Yu L, Zhong C-G,
695 Zhou P-K. TNKS1BP1 functions in DNA double-strand break repair through facilitating DNA-PKcs
696 autophosphorylation dependent on PARP-1. Oncotarget. 2015; 6(9): 7011-7022.
697 35 Tan W, Guan H, Zou LH, Wang Y, Liu XD, Rang WQ, Zhou PK, Pei HD, Zhong CG. Overexpression of
698 TNKS1BP1 in lung cancers and its involvement in homologous recombination pathway of DNA
699 double-strand breaks. Cancer Med. 2017; 6(2):483-493.
700 36 Ohishi T, Yoshida H, Katori M, Migita T, Muramatsu Y, Miyake M, Ishikawa Y, Saiura A, Iemura SI,
701 Natsume T, Seimiya H. Tankyrase-Binding Protein TNKS1BP1 Regulates Actin Cytoskeleton
702 Rearrangement and Cancer Cell Invasion. Cancer Res. 2017; 77(9):2328-2338.
703 37 Villanyi Z, Collart MA. Ccr4-Not is at the core of the eukaryotic gene expression circuitry. Biochem
704 Soc Trans. 2015; 43(6):1253-8.
705 38 Collart MA, Panasenko OO. The Ccr4--not complex. Gene. 2012; 492(1):42-53.
706 39 Miller JE, Reese JC. Ccr4-Not complex: the control freak of eukaryotic cells. Crit Rev Biochem Mol
707 Biol. 2012; 47(4):315-33.
708 40 Lau NC, Kolkman A, van Schaik FM, Mulder KW, Pijnappel WW, Heck AJ, Timmers HT. Human
709 Ccr4-Not complexes contain variable deadenylase subunits. Biochem J. 2009; 422(3):443-53.
710 41 Boland A, Chen Y, Raisch T, Jonas S, Kuzuoğlu-Öztürk D, Wohlbold L, Weichenrieder O, Izaurralde
711 E. Structure and assembly of the NOT module of the human CCR4-NOT complex. Nat Struct Mol Biol.
712 2013; 20(11):1289-97.
713 42 Collart MA. Global control of gene expression in yeast by the Ccr4-Not complex. Gene. 2003;
714 313:1-16.
715 43 Reese JC. The control of elongation by the yeast Ccr4-not complex. Biochim Biophys Acta. 2013;
716 1829(1):127-33.
717 44 Bai Y, Salvadore C, Chiang YC, Collart MA, Liu HY, Denis CL. The CCR4 and CAF1 proteins of the
718 CCR4-NOT complex are physically and functionally separated from NOT2, NOT4, and NOT5. Mol Cell
719 Biol. 1999; 19(10):6642-51.

720 45 Basquin J, Roudko VV, Rode M, Basquin C, Séraphin B, Conti E. Architecture of the nuclease
721 module of the yeast Ccr4-not complex: the Not1-Caf1-Ccr4 interaction. Mol Cell. 2012; 48(2):207-18
722 46 Wahle E, Winkler GS. RNA decay machines: deadenylation by the Ccr4-not and Pan2-Pan3
723 complexes. Biochim Biophys Acta. 2013; 1829(6-7):561-70.
724 47 Doidge R, Mittal S, Aslam A, Winkler GS. Deadenylation of cytoplasmic mRNA by the mammalian
725 Ccr4-Not complex Biochem Soc Trans. 2012; 40(4):896-901.
726 48 Panasenko OO. The role of the E3 ligase Not4 in cotranslational quality control. Front Genet.
727 2014; 5:141. doi: 10.3389/fgene.
728 49 Inada T, Makino S. Novel roles of the multi-functional CCR4-NOT complex in post-transcriptional
729 regulation. Front Genet. 2014; 5:135. doi: 10.3389/fgene.
730 50 Shirai YT, Suzuki T, Morita M, Takahashi A, Yamamoto T. Multifunctional roles of the mammalian
731 CCR4-NOT complex in physiological phenomena. Front Genet. 2014; 5:286. doi: 10.3389.
732 51 Petit AP, Wohlbold L, Bawankar P, Huntzinger E, Schmidt S, Izaurralde E, Weichenrieder O. The
733 structural basis for the interaction between the CAF1 nuclease and the NOT1 scaffold of the human
734 CCR4-NOT deadenylase complex. Nucleic Acids Res. 2012; 40(21):11058-72.
735 52 Bawankar P, Loh B, Wohlbold L, Schmidt S, Izaurralde E. NOT10 and C2orf29/NOT11 form a
736 conserved module of the CCR4-NOT complex that docks onto the NOT1 N-terminal domain. RNA
737 Biol. 2013; 10(2):228-44
738 53 Mulder KW, Winkler GS, Timmers HT. DNA damage and replication stress induced transcription of
739 RNR genes is dependent on the Ccr4-Not complex. Nucleic Acids Res. 2005; 33(19):6384-92.
740 54 Bennett CB, Lewis LK, Karthikeyan G, Lobachev KS, Jin YH, Sterling JF, Snipe JR, Resnick MA. Genes
741 required for ionizing radiation resistance in yeast. Nat Genet. 2001; 29(4):426-34
742 55 Traven A, Hammet A, Tenis N, Denis CL, Heierhorst J. Ccr4-not complex mRNA deadenylase
743 activity contributes to DNA damage responses in Saccharomyces cerevisiae. Genetics. 2005;
744 169(1):65-75.

745 56 Cheng CY, Gilson T, Dallaire F, Ketner G, Branton PE, Blanchette P. The E4orf6/E1B55K E3
746 ubiquitin ligase complexes of human adenoviruses exhibit heterogeneity in composition and
747 substrate specificity. J Virol. 2011; 85(2):765-75.
748 57 Sarnow P, Ho YS, Williams J, Levine AJ. Adenovirus E1b-58kd tumor antigen and SV40 large tumor
749 antigen are physically associated with the same 54 kd cellular protein in transformed cells. Cell.
750 1982; 28(2):387-94
751 58 Levine AJ. The common mechanisms of transformation by the small DNA tumor viruses: The
752 inactivation of tumor suppressor gene products: p53. Virology. 2009; 384(2):285-93.
753 59 DeCaprio JA. How the Rb tumor suppressor structure and function was revealed by the study of
754 Adenovirus and SV40. Virology. 2009; 384(2):274-84.
755 60 White EA, Kramer RE, Tan MJ, Hayes SD, Harper JW, Howley PM. Comprehensive analysis of host
756 cellular interactions with human papillomavirus E6 proteins identifies new E6 binding partners and
757 reflects viral diversity. J Virol. 2012; 86(24):13174-86.
758 61 Ben-Israel H, Kleinberger T. Adenovirus and cell cycle control. Front Biosci. 2002; 7:d1369-95.
759 62 Spitkovsky D1, Jansen-Dürr P, Karsenti E, Hoffman I. S-phase induction by adenovirus E1A
760 requires activation of cdc25a tyrosine phosphatase. Oncogene. 1996; 12(12):2549-54.
761 63 Querido E, Marcellus RC, Lai A, Charbonneau R, Teodoro JG, Ketner G, Branton PE. Regulation of
762 p53 levels by the E1B 55-kilodalton protein and E4orf6 in adenovirus-infected cells. J Virol. 1997;
763 71(5):3788-98.
764 64 Steegenga WT, Riteco N, Jochemsen AG, Fallaux FJ, Bos JL. The large E1B protein together with
765 the E4orf6 protein target p53 for active degradation in adenovirus infected cells. Oncogene. 1998;
766 16(3):349-57.
767 65 Hutchins JR, Toyoda Y, Hegemann B, Poser I, Hériché JK, Sykora MM, Augsburg M, Hudecz O,
768 Buschhorn BA, Bulkescher J, Conrad C, Comartin D, Schleiffer A, Sarov M, Pozniakovsky A, Slabicki
769 MM, Schloissnig S, Steinmacher I, Leuschner M, Ssykor A, Lawo S, Pelletier L, Stark H, Nasmyth K,

770 Ellenberg J, Durbin R, Buchholz F, Mechtler K, Hyman AA, Peters JM. Systematic analysis of human
771 protein complexes identifies chromosome segregation proteins. Science. 2010; 328(5978):593-9.
772 66 Huttlin EL, Ting L, Bruckner RJ, Gebreab F, Gygi MP, Szpyt J, Tam S, Zarraga G, Colby G, Baltier K,
773 Dong R, Guarani V, Vaites LP, Ordureau A, Rad R, Erickson BK, Wühr M, Chick J, Zhai B, Kolippakkam
774 D, Mintseris J, Obar RA, Harris T, Artavanis-Tsakonas S, Sowa ME, De Camilli P, Paulo JA, Harper JW,
775 Gygi SP. The BioPlex Network: A Systematic Exploration of the Human Interactome. Cell. 2015;
776 162(2):425-40.
777 67 Havugimana PC1, Hart GT, Nepusz T, Yang H, Turinsky AL, Li Z, Wang PI, Boutz DR, Fong V, Phanse
778 S, Babu M, Craig SA, Hu P, Wan C, Vlasblom J, Dar VU, Bezginov A, Clark GW, Wu GC, Wodak SJ,
779 Tillier ER, Paccanaro A, Marcotte EM, Emili A A census of human soluble protein complexes. Cell.
780 2012; 150(5):1068-81.
781 68 Dallaire F, Schreiner S, Blair GE, Dobner T, Branton PE, Blanchette P. The Human Adenovirus Type
782 5 E4orf6/E1B55K E3 Ubiquitin Ligase Complex Enhances E1A Functional Activity. mSphere. 2015;
783 1(1). pii: e00015-15. doi: 10.1128/mSphere.00015-15.
784 69 Byrd P, Brown KW, Gallimore PH. Malignant transformation of human embryo retinoblasts by
785 cloned adenovirus 12 DNA. Nature. 1982; 298(5869):69-71
786 70 Barker DD, Berk AJ. Adenovirus proteins from both E1B reading frames are required for
787 transformation of rodent cells by viral infection and DNA transfection. Virology. 1987; 156(1):107-21.
788 71 Halbert DN, Cutt JR, Shenk T. Adenovirus early region 4 encodes functions required for efficient
789 DNA replication, late gene expression, and host cell shutoff. J Virol. 1985; 56(1):250-7.
790 72 Miron MJ, Blanchette P, Groitl P, Dallaire F, Teodoro JG, Li S, Dobner T, Branton PE. Localization
791 and importance of the adenovirus E4orf4 protein during lytic infection. J Virol. 2009; 83(4):1689-99.
792 73 Blanchette P, Kindsmüller K, Groitl P, Dallaire F, Speiseder T, Branton PE, Dobner T. Control of
793 mRNA export by adenovirus E4orf6 and E1B55K proteins during productive infection requires E4orf6
794 ubiquitin ligase activity. J Virol. 2008; 82(6):2642-51.

795 74 Byrd PJ, Grand RJ, Breiding D, Williams JF, Gallimore PH. Host range mutants of adenovirus type
796 12 E1 defective for lytic infection, transformation, and oncogenicity. Virology. 1988; 163(1):155-65.
797 75 Rubenwolf S, Schütt H, Nevels M, Wolf H, Dobner T. Structural analysis of the adenovirus type 5
798 E1B 55-kilodalton-E4orf6 protein complex. J Virol. 1997; 71(2):1115-23.

799

800 **Figure legends**

801 **Figure 1: The Degradation of Tab182 following infection with adenovirus serotype 5 or adenovirus**
802 **serotype 12 is dependent on the adenovirus E1B55K protein.** HeLa cells were infected with
803 adenovirus serotype 5 (A), or serotype 12 (B) at 5 pfu/cell. HeLa cells were also infected with
804 adenovirus serotype 5 E1B55K negative virus Ad5dl1520 (C), and adenovirus serotype 12 E1B55K
805 negative virus Ad12dl620 (D) at 10 pfu/cell. Cells were then harvested at various time points (0, 8,
806 24, 48, 72 and 96 hours) post-infection. Cell lysates were subjected to SDS-PAGE and Western
807 blotting using the indicated antibodies.

808 **Figure 2: The Degradation of Tab182 following infection with adenovirus serotype 5 is dependent**
809 **on the adenovirus E4orf6 protein.** HeLa cells were infected with Ad5 E4 mutants H5*in*351 (E4orf1-)
810 **(A)**, H5*pm*4154 (E4orf6-) **(A)**, H5*pm*4155 (E4orf3-E4orf6-) **(B)**, H5*pm*4166 (E4orf4-) **(B)**, H5*dl*356
811 (E4orf6-E4orf7-) **(C)** H5*in*352 (E4orf2-) **(C)** and H5*pm*4150 (E4orf3-) (**D**) at 10 pfu/cell. Cells were then
812 harvested at various time points (0, 8, 24, 48, 72 and 96 hours) post-infection. Cell lysates were
813 subjected to SDS-PAGE and Western blotting using the indicated antibodies.

814 **Figure 3: Tab182 gene expression is enhanced in adenovirus infected cells.** HeLa cells
815 were infected with Ad5 or Ad12 at 5 pfu/cell. Cells were harvested at various time points (0,
816 8, 24, 48, 72 and 96 hours) post-infection. Cellular RNA was extracted from Ad5 (**A**) and
817 Ad12 (**B**) infected cells and first-strand cDNA synthesis carried out. The RT-PCR reactions
818 were performed using Tab182-specific primers and real-time PowerUp™ SYBR® Green
819 Master Mix. To determine the relative Tab182 gene expression, calculated Tab182 Ct values
820 were normalized to Ct values of GAPDH amplified from the same sample [ΔCt = Ct (Tab182)

821 − Ct (GAPDH)], and the 2−ΔΔCt method was used to calculate relative expression. Each
822 experiment was performed in triplicate. . Western blots of the Ad5 and Ad12 infected HeLa cells
823 were performed to confirmTab182 degradation (data not shown).
824

825 **Figure 4: The Degradation of Tab182 during adenovirus serotype 5 and 12 Infection is dependent**
826 **on the adenovirus E1B55K and E4orf6 proteins.** 2 µg of plasmid DNA as shown was transfected into
827 HeLa cells and 48 hours later cells were harvested and subjected to SDS-PAGE and Western blotting
828 using the indicated antibodies. Ad5 and Ad12 E4orf6 proteins were detected with an antibody which
829 recognised the HA tag. GAPDH is included as a loading control.

830 **Figure 5: Tab182 level following infection by Group B, D and E adenoviruses.** HeLa cells were
831 infected with: (**A**) Ad5 (group C) and Ad12 (group A), (**B**) Ad4 (group E) and Ad9 (Group D), and (**C**)
832 Ad11 (group B2) and Ad7 (group B1) at 5 pfu/cell. Cells were harvested at 8, 24, 48, 72, 96 and 120
833 hours post infection. Cell lysates were subjected to SDS-PAGE and Western blotting using antibodies
834 against Tab182, MRE11, p53 and β-actin. Hexon expression was confirmed, as a marker of viral
835 infection, by Ponceau S staining of Western blots for total protein.

836 **Figure 6: The down-regulation of Tab182 protein levels during Ad5 and Ad12 infection can be**
837 **rescued by the proteasomal inhibitor Bortezomib.** HeLa cells were infected with Ad5 (**A**) or Ad12 (**B**)
838 at 5 pfu/cell. Cells were treated with 0.5 µM Bortezomib or DMSO control and harvested after 48
839 hours. Cell lysates were subjected to SDS-PAGE and Western blotting using the indicated antibodies.

840 **Figure 7: The Degradation of Tab182 during Ad5 and Ad12 infection is dependent on cullin**
841 **function.** HeLa cells were infected with Ad5 and Ad12 at 5 pfu/cell. Cells were treated with the
842 Nedd8 inhibitor MLN4924 (4 µM) 1 hour before infection and retreated immediately post-infection.
843 Cells were harvested at various time points (0, 8, 24, 48, 72 and 96 hours) post-infection. Cell lysates
844 were subjected to SDS-PAGE and Western blotting using the indicated antibodies (**A**) and (**B**). H1299
845 cells **(C)** or H1299 cells with ablation of Cul2 **(D)** or Cul5 **(E)** expression were infected with either Ad5

or Ad12 and harvested at 0, 8, 24, 48, 72 and 96 hours post-infection. Cell lysates were subjected to SDS-PAGE and Western blotting with the antibodies shown.

Figure 8: Tab182 does not localise to viral replication centres during adenovirus infection. GFP-Tab182 was transfected into HeLa cells and 24 hours later cells were infected with Ad5 or Ad12. (**A**), 30 hours later cells were fixed, extracted and probed with the appropriate antibodies. (**B**) 30 hours after infection cells were pre-extracted as described in the Materials and Methods section before fixing and then staining with antibodies. In both (**A**) and (**B**) Ad5 infected cells were probed with DBP antibody, whilst Ad12 infected cells were probed with RPA32 antibody. Nuclear DNA is stained with DAPI.

Figure 9: Adenovirus early region E1B55K interacts with Tab182 *in vitro* and *in vivo.* Ad12E1HER2 **(A)** and Ad5E1HEK293 **(B)** cell lysates containing 500 µg total protein were incubated with 5 µg either GST-Tab182, GST-PRMT1 or with GST alone. Protein complexes were captured by glutathione-agarose beads, subjected to SDS-PAGE and Western blotting with the antibodies indicated. Ad5E1HEK293 **(C)** and Ad12E1HER2 **(D)** cell lysates (500 µg total protein) were incubated with antibodies against Tab182, collagen IV together with IgG (non-specific binding controls). Immuno-complexes were isolated using Protein-G agarose beads and subsequently resolved by SDS-PAGE and Western blotting using antibodies against Ad5/Ad12 E1B55K proteins. **(E)** GFP-Tab182 was transfected into Ad5E1HEK293 and Ad12E1HER2 cell lines which were harvested after 48 hours. Cell lysates (500µg total protein) were incubated with Ad5 and Ad12 E1B55K antibodies together with IgG. Western blotting was with an antibody against Tab182. (**F**) HeLa cells were transfected with pcDNA3 or pcDNA3 constructs expressing HA-tagged Ad9E1B55K or Ad16E1B55K. After 48hours lysates (500µg total protein) were immunoprecipitated with an antibody against Tab182 or rabbit IgG. Western blotting was with an antibody against HA. (**G**) is an over-exposed version of a portion of the western blot shown in (**F**). (**H**) Ad5E1HEK293 cells were transfected with pcDNA3 or pcDNA3 constructs expressing HA-tagged Ad9E1B55K or Ad16E1B55K. After 48hours lysates (500µg total protein) were immunoprecipitated with an antibody against HA or mouse IgG. Western blotting was

with an antibody against p53. (**I**) 293FT cell lysates (500µg protein) were incubated with antibodies against Tab182, collagen IV or IgG control. Western blotting was with an antibody against SV40 T antigen. Ad5E1HEK293 **(J)** and Ad12E1HER2 **(K)** cell lysates (500 µg total protein) were incubated with antibodies against CNOT1, collagen IV together with IgG. Western blotting was with antibodies against Ad5/Ad12 E1B55K proteins. In all cases the whole cell lysates contained 15 µg of protein. Although only limited areas of the western blots are shown no additional bands were seen in the original autoradiographs.

Figure 10: Adenoviruses 5 and 12 degrade components of the CNOT complex. HeLa cells were infected with adenovirus serotype 5 (**A**) or 12 (**B**) at 5 pfu/cell. Cells were harvested at 0, 8, 24, 48, 72 and 96 hours post infection, subjected to SDS-PAGE and Western blotting using the indicated antibodies.

Figure 11: AdE1A protein expression is enhanced in adenovirus-infected, Tab182- or CNOT1-depleted cells. HeLa cells were transfected with control, Tab182 or CNOT1 siRNAs. 48 hours later, control, Tab182 and CNOT1 siRNA treated cells were infected with adenovirus serotype 5 (**A**) or serotype 12 (**B**) at 5 pfu/cell. Cells were then harvested at various time points (0, 8, 24, 48, 72 and 96 hours) post-infection. Cell lysates were subjected to SDS-PAGE and Western blotting using the indicated antibodies.

Figure 12: Expression of cyclin E and is enhanced in Tab182 and CNOT1 depleted cells. HeLa cells were transfected with control, Tab182 or CNOT1 siRNAs. 48 hours later, control, Tab182 and CNOT1 siRNA treated cells were mock infected (**A**) or infected with adenovirus serotype 12 (**B**) at 5 pfu/cell. Cells were then harvested at various time points (0, 8, 24, 48, 72 and 96 hours) post-infection. Cell lysates were subjected to SDS-PAGE and Western blotting using the indicated antibodies.

Figure 13: The relative expression of Ad13S E1A mRNA is increased in infected cells in the absence of CNOT1 or Tab182. HeLa cells were transfected with control, Tab182 or CNOT1 siRNAs and 48 hours later infected with Ad5 (**A**) or Ad12 (**B**) at 5 pfu/cell. Cellular RNA was extracted from infected cells and first-strand cDNA synthesis carried out. The RT-PCR reactions were performed using

898 Ad13SE1A CR3 region specific primers and real-time PowerUp™ SYBR® Green Master Mix. To check
899 E1A relative gene expression, calculated E1A Ct values were normalized to Ct values of GAPDH
900 amplified from the same sample [ΔCt = Ct (E1A) − Ct (GAPDH)], and the 2−ΔΔCt method was used to
901 calculate relative gene expression. Data are the mean of 3 repeats. The statistical significance was
902 determined using Student's *t*-test, p-values less than 0.05 (*) or 0.01 (**) were considered
903 significant. Error bars represent SEM.

904 **Figure 14: Viral DNA synthesis is increased in Tab182 and CNOT1-depleted cells after adenovirus**
905 **infection.** HeLa cells were treated with control, Tab182 and CNOT1 siRNA for 48 hours and then
906 infected with Ad5 (**A**) or Ad12 (**B**) at 5 pfu/cell. After 24 hours cells were harvested and the total DNA
907 isolated. Quantitative PCR was performed to determine relative concentration of viral DNA. Hexon
908 Ct values were normalized to Ct values for GAPDH DNA amplified from the same sample. Data are
909 the mean of 3 repeats. The statistical significance was determined using Student's *t*-test, p-values
910 less than 0.05 (*) or 0.01 (**) were considered significant. Error bars represent SEM.

911

912

913

914

915

916 **Legend to Table 1**

917 **Table1 Proteins identified by mass spectrometric analysis after co-immunoprecipitation with**
918 **Tab182 antibody.** HeLa cells were immunoprecipitated with a rabbit antibody raised against the C-
919 terminal fragment of Tab182 and analysed as described in the Methods section. These data are
920 representative of five independent experiments.

921 **Table 2 Primers used in this study**

922

923 **Table1**

Protein	Peptide	Percentage	Mascot Score

	number	coverage	
Tab182	68	49.4	3491
CCR4-NOT1	38	17.4	1472
CCR4-NOT3	7	10.2	237
CCR4-NOT7	6	28.8	211
CCR4-NOT2	5	12.2	245
CCR4-NOT6L	1	1.8	21
CCR4-NOT10	1	1.3	29
C2orf29 (NOT11)	1	2.4	56
RCD1 (NOT9)	6	20.4	224
PRMT3	9	18.5	377
FHL2	12	52.3	470

924

925 **Table 2**

Gene	Sequence (5'->3') Forward primer Reverse primer	Length	Start	Stop	Product Size (bases)
E1A-Ad5 (CR3)	TAGATTATGTGGAGCACCCCG GCCACAGGTCCTCATATAGCAA	21 22	990 1099	1010 1078	110
E1A-Ad12 (CR3)	AGTCCTGTGAGCACCACCG GTAGGCTCGCAGATAGCACA	19 20	980 998	1053 1034	74
Tab182	CTGCTCTGAGGGACTCCTTG CTGGGTCTCCTCTAGGGCTT	20 20	2310 2448	2329 2467	158
GAPDH (RNA)	GAGTCAACGGATTTGGTCGT ACAAGCTTCCCGTTCTCAG	20 19	53 218	72 236	183
GAPDH (DNA)	CGGCTACTAGCGGTTTTACG AGAAGATGCGGCTGACTGT	20 20	6534369 6534538	6534388 6534557	188
Hexon-Ad5	GCCACGGTGGGGTTTCTAAACTT GCCCCAGTGGTCTTACATGCACATC	23 25	18862 18967	18882 18989	127
Hexon-Ad12	GCCACGGTGGGGTTTCTAAACTT GCCCCAGTGGTCTTACATGCACATC	23 25	17764 17869	17784 17891	127

926

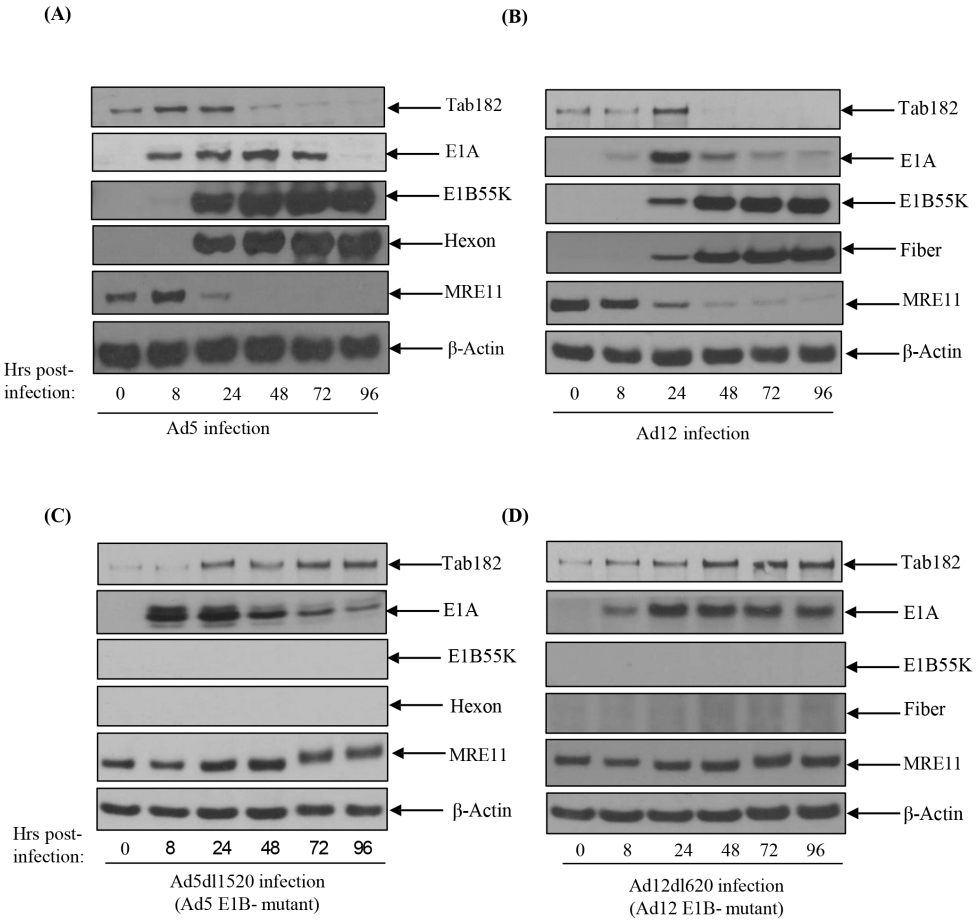

Figure 1

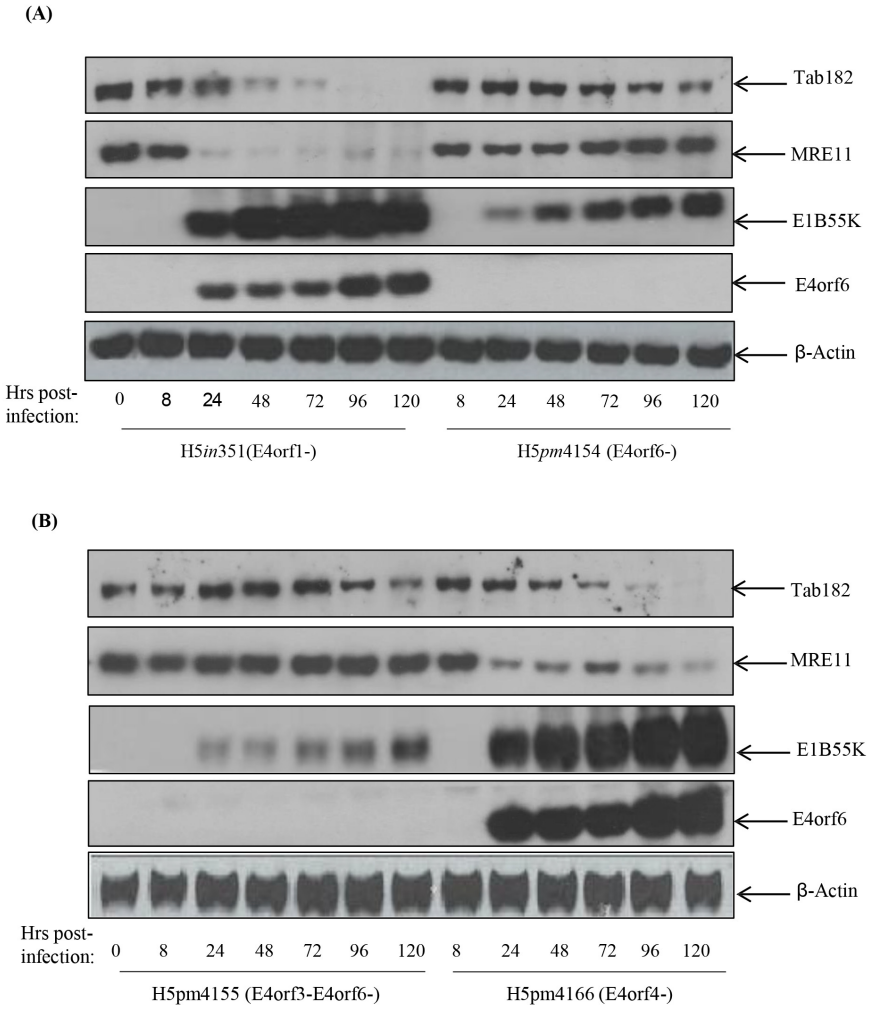

Figure 2

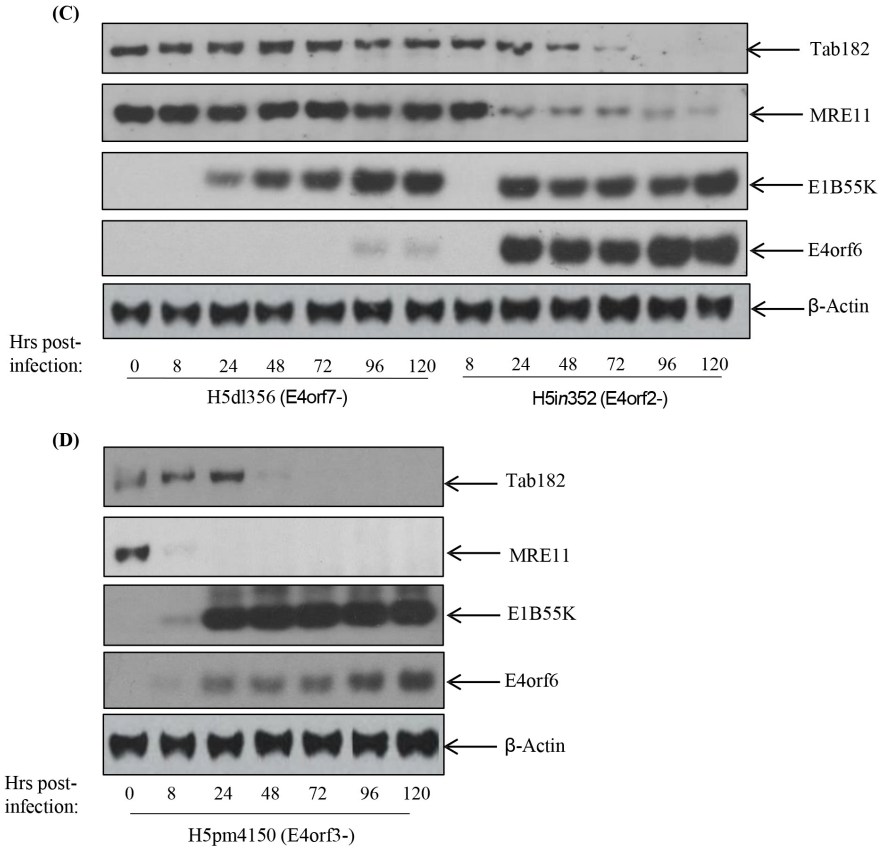

Figure 2

(A)

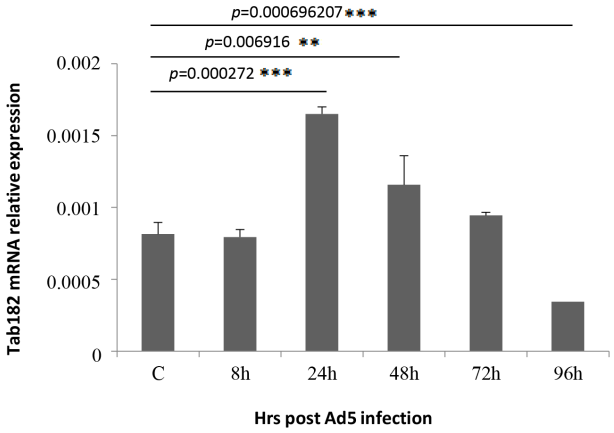

(B)

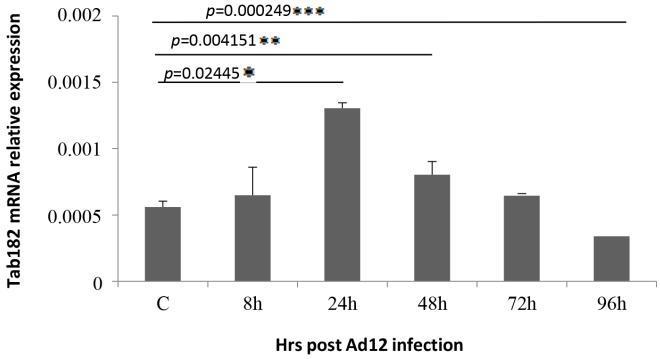

Figure 3

Figure 4

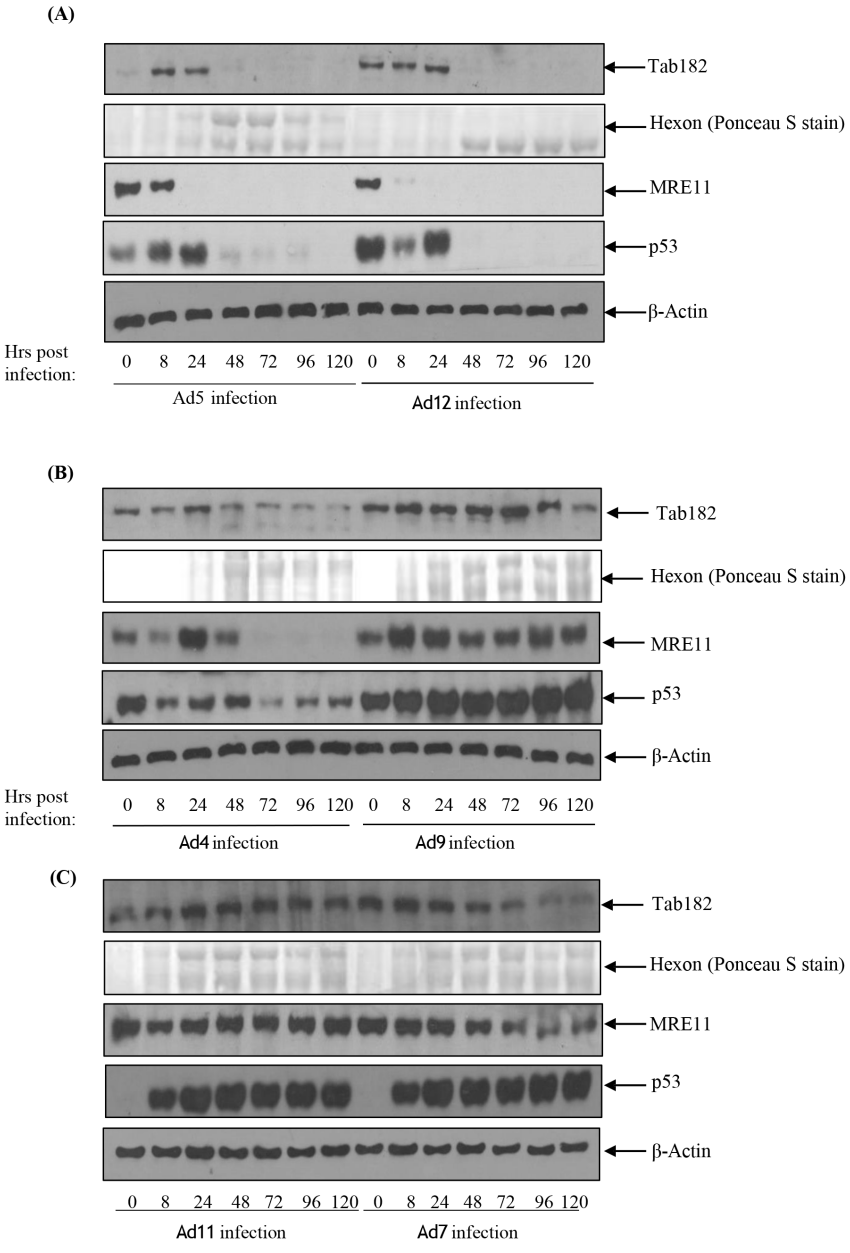

Figure 5

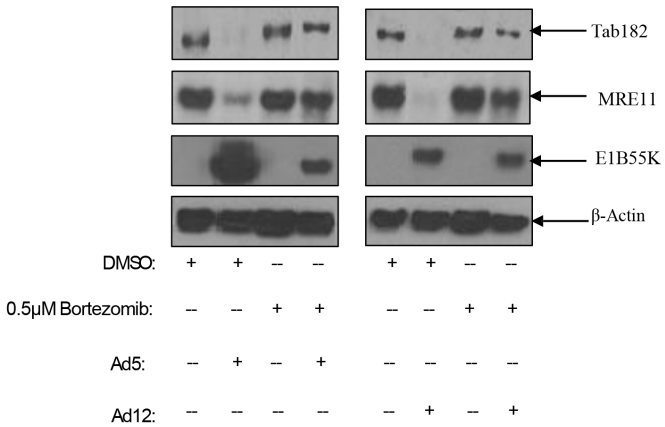

Figure 6

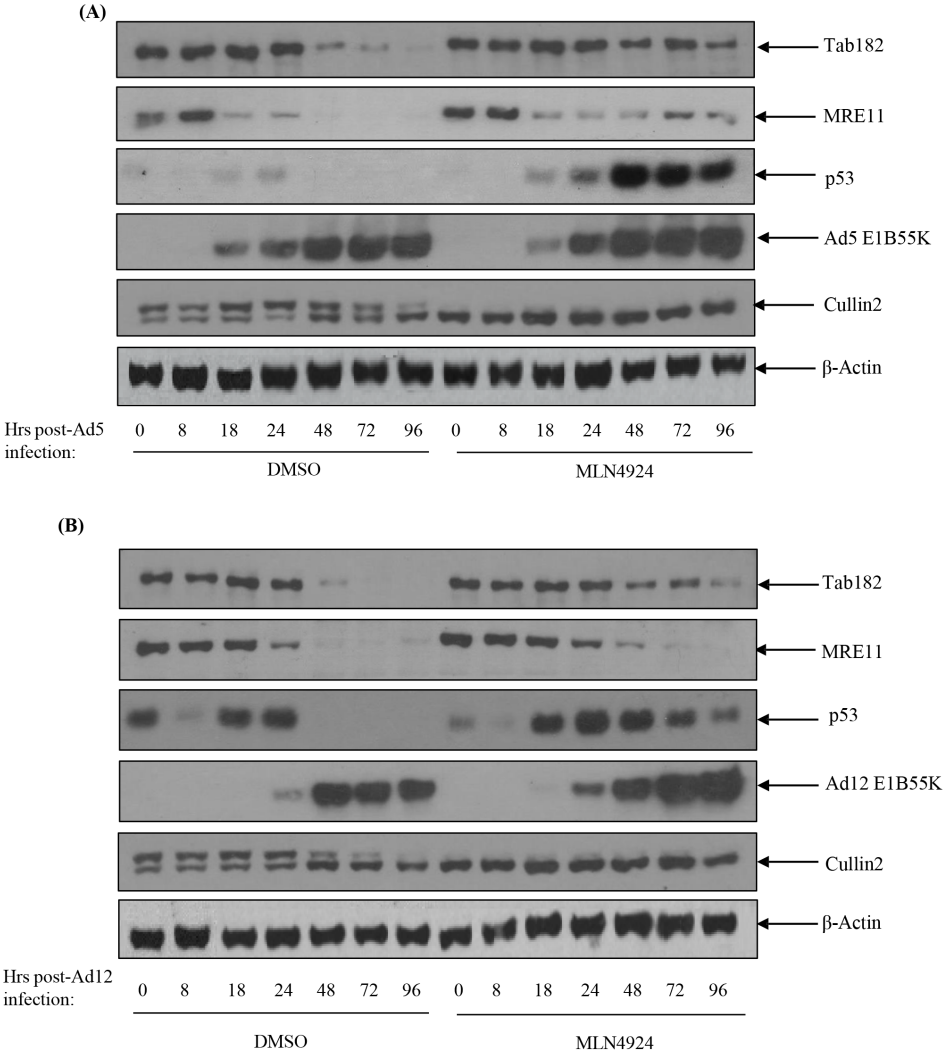

Figure 7

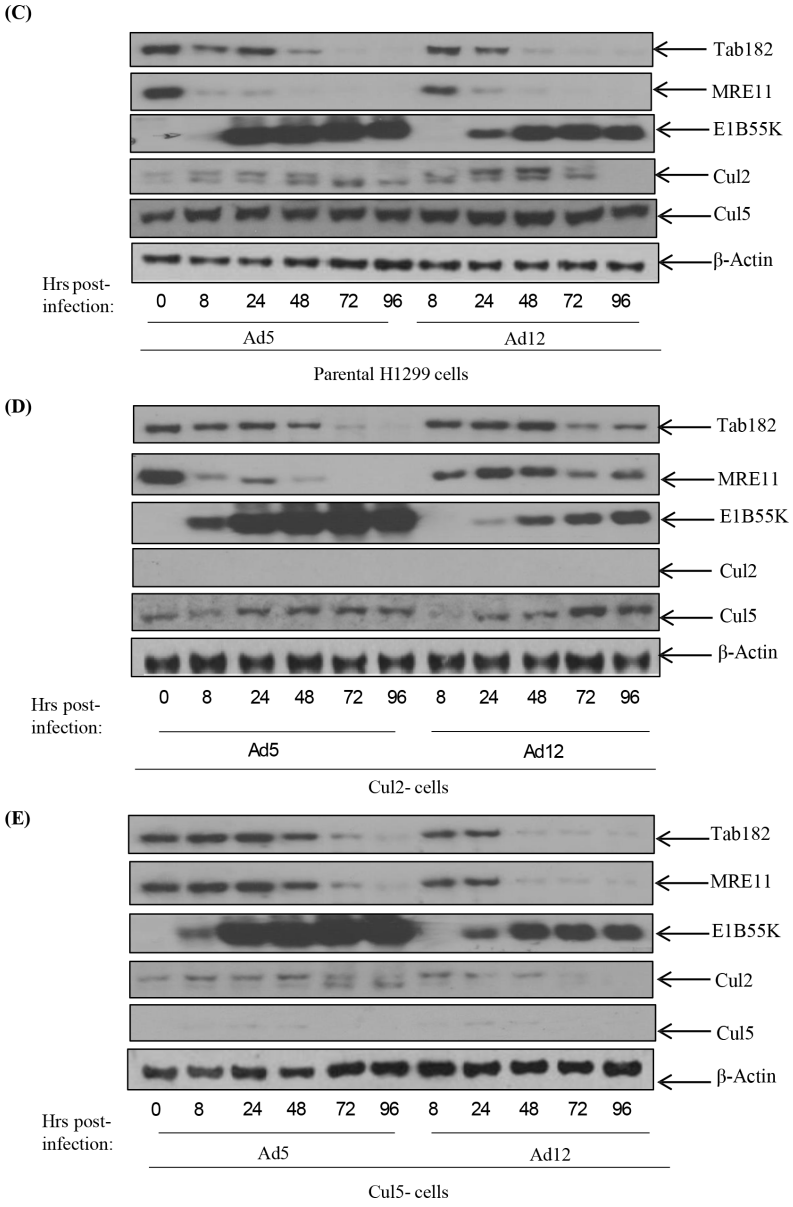

Figure 7

Figure 8

Figure 9

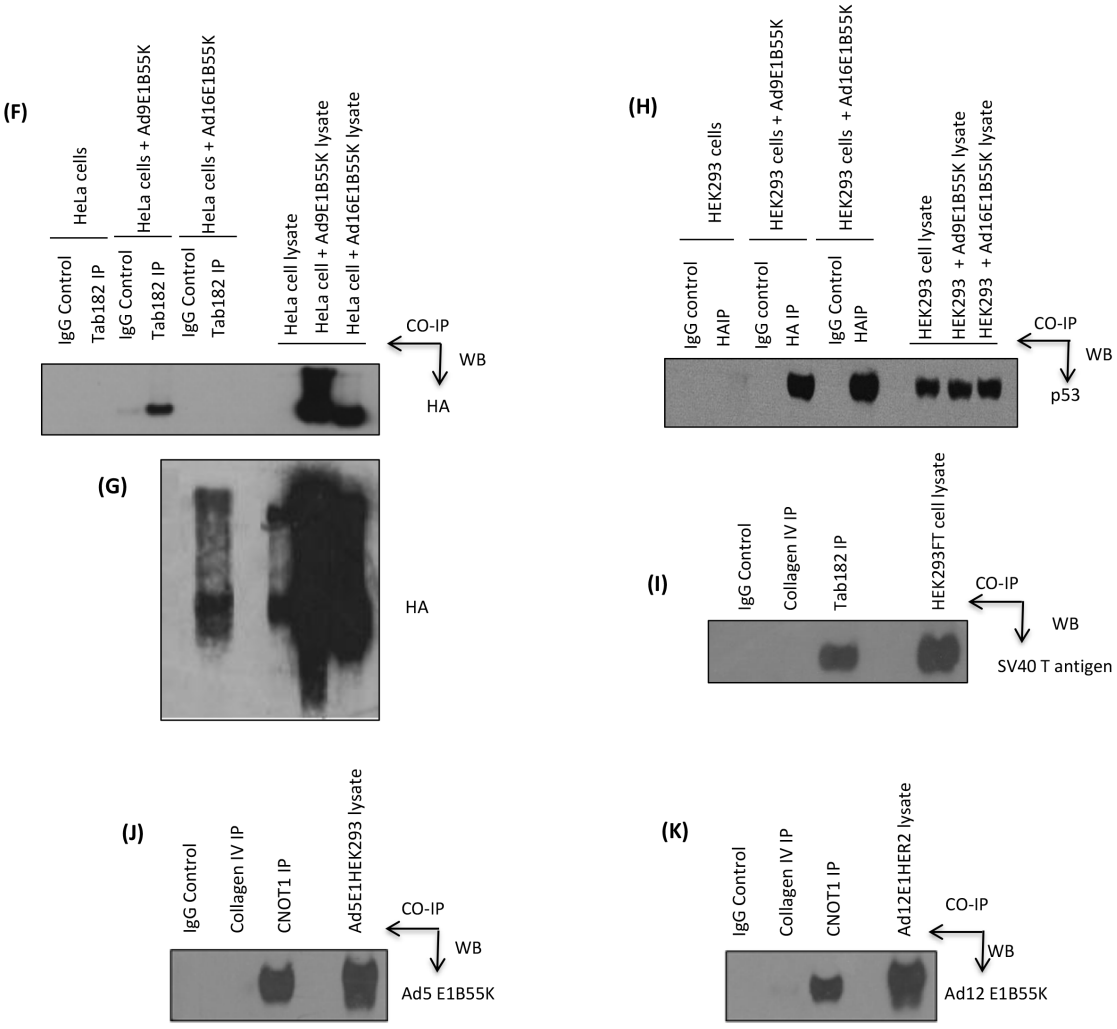

Figure 9

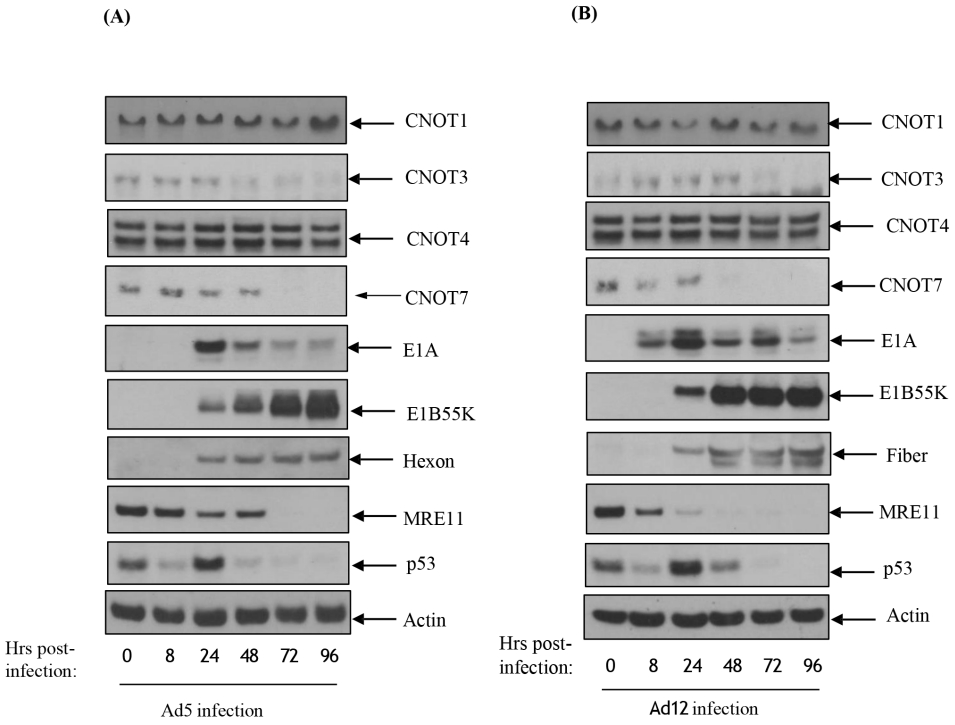

Figure 10

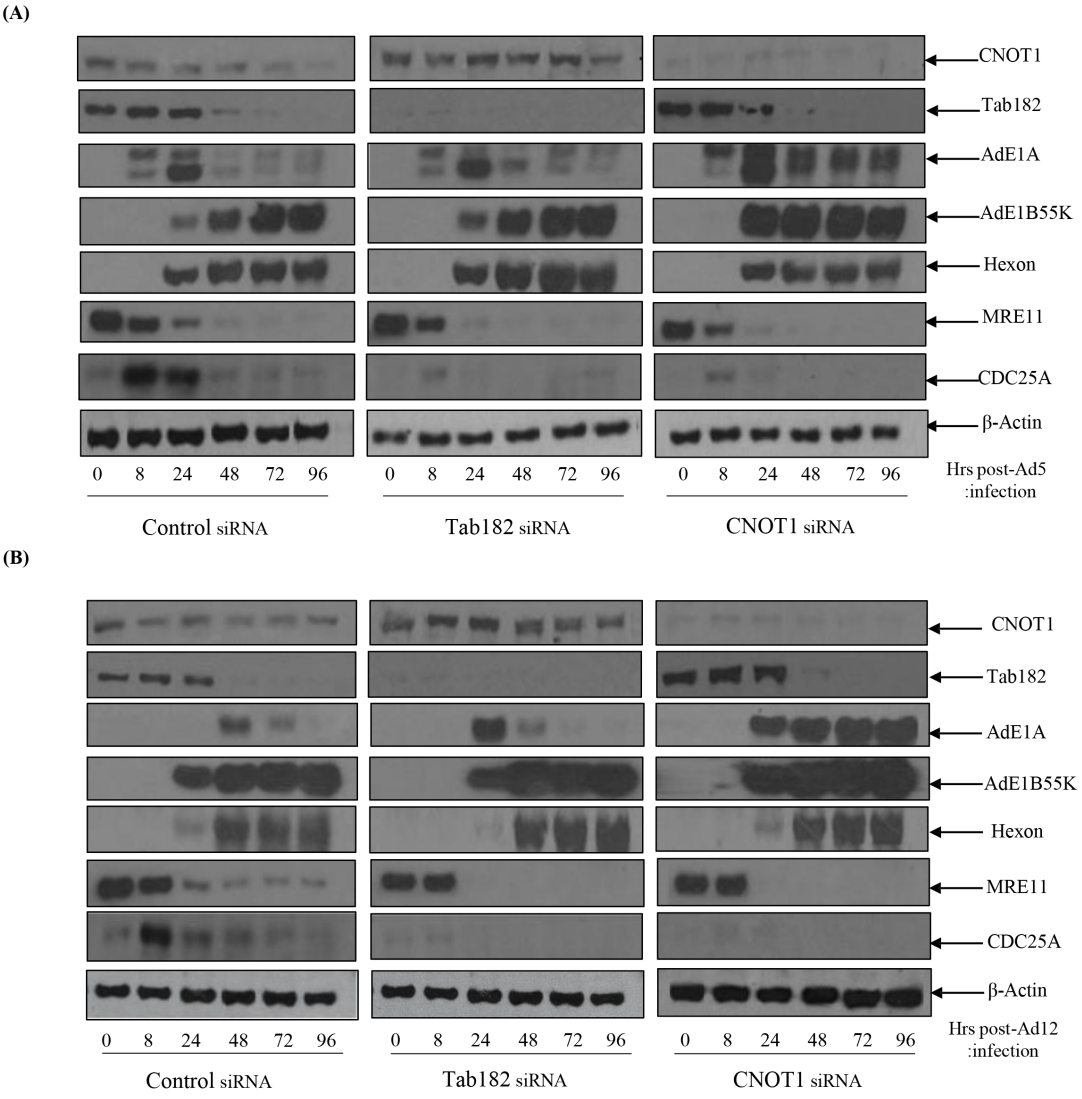

Figure 11

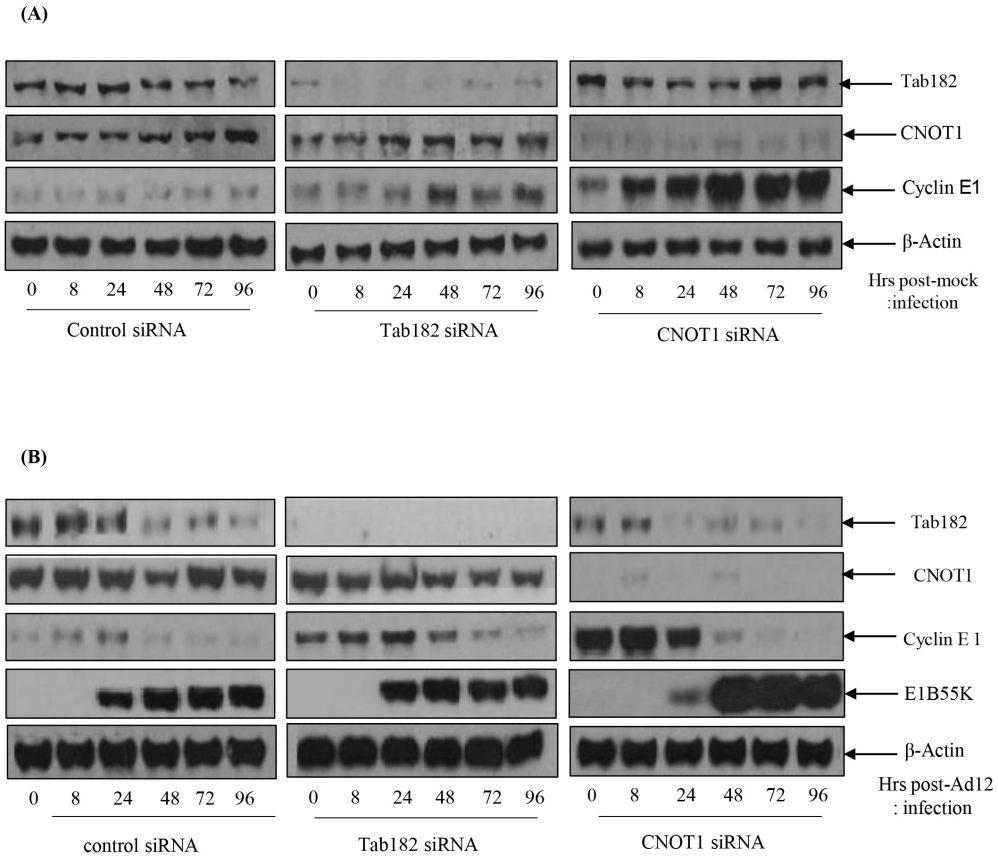

Figure 12

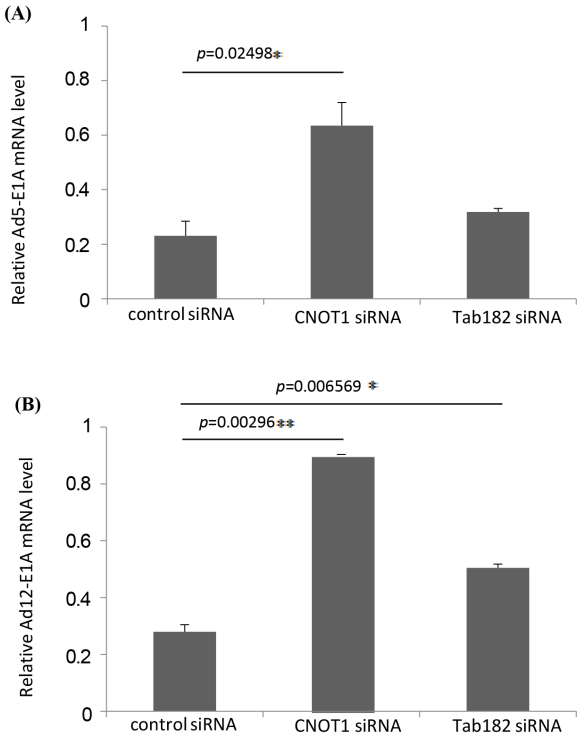

Figure 13

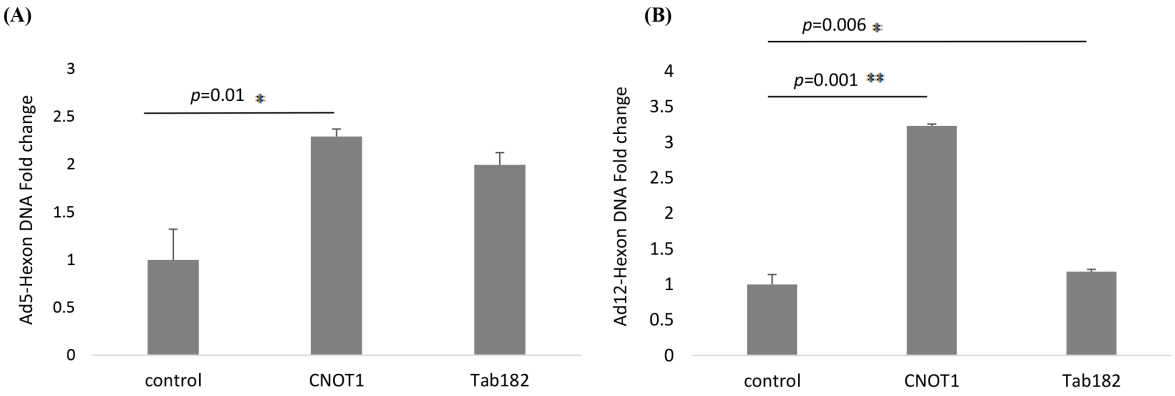

Figure 14